IMPERIAL COLLEGE LONDON

Department of Earth Science and Engineering

Centre for Petroleum Studies

Analysis of down-hole temperature response to determine flow rates in producing zones

By

Emre Cengiz

A report submitted in partial fulfillment of the requirements for the MSc and/or the DIC.

September 2013

DECLARATION OF OWN WORK

I declare that this thesis: “Analysis of down-hole temperature response to determine flow rates in producing zones” is entirely my own work and that where any material could be construed as the work of others, it is fully cited and referenced, and/or with appropriate acknowledgement given.

Signature:...

Name of student: Emre Cengiz

Name of supervisors: Prof. Martin Blunt
Amit Madahar

Abstract

Knowing the contribution of different producing layers to total flow rate is vital for effective reservoir management and project economics. This can be measured production logging with spinner flow meter or analyzing flowing fluid temperature response by using energy balance between flowing fluid and the surrounded formation. Heat exchange between the produced fluid and surrounded formation is a function of mass flow rate, time of production, fluid gravity, geothermal gradient and various thermal coefficients thus, the flowing fluid temperature can be useful in quantifying the flow rate from each reservoir layer. Flowing fluid temperature can be measured by dynamic temperature logging or permanently installed fiber optic cables called distributed temperature sensing (DTS). Contrary to conventional production logging methods, calculating flow rates using temperature measurements offers real time production monitoring without any restrictions.

This study provides an analysis of the temperature profile to calculate the flow contributions from different reservoir layers and discusses its applicability in real scenarios by analyzing conventional dynamic temperature logging and high resolution DTS data. Temperature data were analyzed by modified form of Ramey's pioneering model (1962) and the commercial software THERMA. Thereafter the consistency of the analysis for selected field cases are compared with flow rates determined from spinner flow meters. As a result of analysis; the contribution of different production layers are calculated and some production problems such as flow behind casing are identified by using flowing fluid temperature measurements.

Acknowledgements

I would like to express the deepest appreciation to Professor Martin Blunt, who has the attitude and the substance of a genius: he continually and convincingly conveyed a spirit of adventure in regard to this thesis project and an excitement in regard to teaching. Without his guidance and persistent help this dissertation would not have been possible.

A special gratitude I give to Mr. Amit Madahar, who introduced me to the topic of this thesis project, helped me to coordinate my project.

I wish to thank Mr. George Brown, for providing me his excellent thermal modeling and analysis software THERMA.

I would like to thank my family who believed and encouraged me during the year in Imperial College. I would not be able to finish this course without their support.

I also would like to thank my fiancé, Merve Celikkan. She was always there cheering me up and stood by me through the good times and bad

Last but not least, I also express my deepest gratitude to Prof. Alain Gringarten for his extensive knowledge, teaching and understanding on me during the year in Imperial College.

“If we knew what it was we were doing, it would not be called research, would it?”
Albert Einstein

Table of Contents

List of Figures

List of Tables

Imperial College London

Analysis of down-hole temperature response to determine flow rates in producing zones

Emre Cengiz

Imperial College Supervisor: Prof. Martin Blunt
Industry Supervisor: Amit Madahar-Petrovision Energy Services

Abstract

Knowing the contribution of different producing layers to total flow rate is vital for effective reservoir management and project economics. This can be measured production logging with spinner flow meter or analyzing flowing fluid temperature response by using energy balance between flowing fluid and the surrounded formation. Heat exchange between the produced fluid and surrounded formation is a function of mass flow rate, time of production, fluid gravity, geothermal gradient and various thermal coefficients thus, the flowing fluid temperature can be useful in quantifying the flow rate from each reservoir layer. Flowing fluid temperature can be measured by dynamic temperature logging or permanently installed fiber optic cables called distributed temperature sensing (DTS). Contrary to conventional production logging methods, calculating flow rates using temperature measurements offers real time production monitoring without any restrictions.

This study provides an analysis of the temperature profile to calculate the flow contributions from different reservoir layers and discusses its applicability in real scenarios by analyzing conventional dynamic temperature logging and high resolution DTS data. Temperature data were analyzed by modified form of Ramey's pioneering model (1962) and the commercial software THERMA. Thereafter the consistency of the analysis for selected field cases are compared with flow rates determined from spinner flow meters. As a result of analysis; the contribution of different production layers are calculated and some production problems such as flow behind casing are identified by using flowing fluid temperature measurements.

Introduction

The importance of the well bore temperature measurement was highlighted by Schlumberger, the pioneer of down-hole measurements- in early 1937(Schlumberger et al. 1937). Temperature logs have been used to understand temperature distributions of formations, however, it is possible to gain more information from the temperature distribution of flowing fluid as a function of depth and time. Temperature logs can be applied to a great number of oil-field problems, both in wells in thermal equilibrium and thermal evolution, and in both open and cased holes (Schlumberger, et al. 1937). Dynamic temperature logs measure the well bore temperature while produced fluid flows. This temperature response of flowing fluid is related to fluid properties, geothermal gradient and heat exchange with surroundings of the well and flow rate.

In both production and injection wells, heat transfer occurs between the flowing fluid and surroundings, such as tubing, casing, cement and formation. When fluid is produced, in most of the cases fluid temperature is equal to the produced zone temperature; however, there can be cooling or heating effect due to the Joule Thompson Effect (JTE). Heat transfer occurs between produced or injected fluids and earth due to temperature difference between these elements while fluid moves in the wellbore. The temperature difference between the wellbore fluid and surroundings, or fluid entry from different producing zones, can account for heat transfer. Since the fluid produced is at a greater temperature than the surroundings, it loses heat to the formation whilst flowing up the wellbore and thus, the produced fluid loses heat throughout the wellbore until it reaches the surface. During production, the hot wellbore fluid provides a source of heat to the formation while, during fluid injection the wellbore acts as a heat sink (Hasan& Kabir, 2002).

The temperature distribution has been modelled for gas and water injection wells by Nowak (1953). After this studied, Ramey (1962) published a theoretical model to estimate the temperature distribution in injection wells. Curtis and Witterholt (1973) modified Ramey's model to producing wells. Ramey's pioneering work led to many developments on many temperature models were developed to estimate temperature profiles in both production and injection models (Ouyang, 2005; Hasan et al. 2007). In the literature on temperature logging, relationships exist which may be used to predict temperature responses in producing wells as a function of volumetric flow rate, time of production, fluid gravity, geothermal gradient and various geothermal coefficients. These relationships indicate that under "ideal conditions" the temperature curve recorded above producing zone as a function of depth exponentially approaches an asymptote parallel to natural geothermal profile (Curtis& Witterholt, 1972). Applying Ramey's model to the production well, it is possible to estimate the flow rate from the corresponding temperature response.

In the last decade, conventional dynamic temperature logging has been replaced by fiber optic cable measurements called Distributed Temperature Sensing (DTS) which is attached to production string with a control line generally ½ inch diameter and measure temperature response of the wellbore every meter by analysing backscattered Raman wavelength light from pulsed laser source. Because the temperature measurements are taken continuously, it is possible to monitor how production is changing as a consequence of changing reservoir conditions. High resolution DTS data has been used to calculate flow contribution in both oil and gas wells to evaluate completion integrity, water injection profiles, and the effectiveness of fracture jobs and to identify wellbore problems such as cement integrity, cross-flow, flow behind casing and other wellbore related events. Many successful applications have been reported using a DTS system to determine the flow profile in the wellbore (Brown et al. 2005; Pinzon, et al. 2007).

As a result of developing measurement technology, some commercial software has been able to simulate the temperature response accounting for zonal contributions from different production zones and hence, this technology can replace conventional production logging techniques. Conventional production logging tools are not effectively applicable at high flow rates and reduced the flow rates impacts on both production and project economics. Also, in some cases, well head configuration should be modified and requires extra space for production logging tool (PLT) operations which could be very difficult in offshore environment. Additionally, PLT still needs improvement for extended reach highly deviated or horizontal wells.

Schlumberger has developed thermal modelling and analysis software (THERMA) that uses a steady state pressure model together with a transient thermal solution that can model most black oil scenarios to facilitate analysis of DTS temperature data. This model has been used to analyse field data (Brown et al. 2005). This study investigated the link between temperature measurements in the wellbore and zonal flow rate by using the model modified by Curtis and Witterholt (1973) for conventional temperature log analysis and employed the software THERMA for complex well schematics.

However, despite the long history of temperature measurements and widespread acknowledgement of their value in production monitoring, the use of such information to determine flow rates is still rare. In this paper, the underlying theory and application to field data will be presented. Field data will be studied using both analytical expressions and commercial software to demonstrate the power of this technique to determine flow rates.

Methodology to model heat transport analytically

Flowing Fluid Temperature

The analysis of temperature distributions in wellbores applies standard physical approaches – namely conservation of energy and the Laplace law for heat conduction – while borrowing many concepts from standard pressure transient analysis. Mathematically the equations are similar to those used in well-test analysis and the analysis is essentially similar to the study of a radial flow period, except that we consider heat fluxes and temperature, rather than Darcy flow and pressure.

The expression for flowing fluid temperature can be derived from energy conservation assuming that physical and thermal properties of both earth and flowing fluid do not change with temperature; heat transfer is rapid in wellbore and radial in the formation. Therefore, the general energy equation is follows (Ramey, 1962).

$$dH + \frac{gdz}{g_c J} + \frac{udu}{g_c J} = dQ_t - \frac{dW_f}{J} \quad \text{.......(1)}$$

Since the flowing fluid is single phase incompressible liquid with constant boundaries, the *Wf* term and kinetic energy term becomes zero and the general energy equation can be simplified as

$$dH + \frac{gdz}{g_c J} = dQ_t \quad \text{.......(2)}$$

Using the definition of enthalpy and assuming the change in enthalpy due to pressure change in well bore equals to change in potential energy the total energy equation forms

$$cdT = dQ_t \quad \text{.......(3)}$$

Assuming no phase change, heat rate lost by the mass of fluid is equals to heat transferred to unit area of casing wall. Therefore this equals to heat rate between casing wall and the formation which can be expressed as a function of dimensionless time

$$dq = -WcdT_f = 2\pi r_{to} U(T_f - T_{co})dz = \frac{2\pi k(T_{co} - T_e)dz}{f(t)} \quad \text{.......(4)}$$

Under the assumption of radial heat transfer and steady flow, dimensionless time function as represented in log linear form as a function of casing outer radius, thermal diffusivity of earth and time. This approximation is valid for most cases more than one week for injection and one hundred days for production; however, there can be inconsistencies at early time (Nowak, 1953).

$$f(t) \approx -ln\left(\frac{r_{ci}}{2\sqrt{\alpha t}}\right) - 0.29 \quad (5)$$

Finally, these equations are solved to find the expression for single phase flowing fluid temperature for injection is defined by Ramey (1962) as follows. A detailed explanation and derivation of the formula provided in **Appendix C.**

$$T_f(z,t) = T_{GS} + g_G z - g_G A + \left[T_0(t) + g_G A - T_{GS}\right]e^{-z/A} \quad (6)$$

The first two terms in the equation represent the geothermal temperature change, while the third term accounts for the displacement between the geothermal gradient and the asymptote. The last term in the equation defines the exponential behaviour of the equation by falling off the terms in brackets while z increases.

$$A = \frac{Wc\left[k + r_{ci}Uf(t)\right]}{2\pi r_{ci}kU} \quad (7)$$

This expression is modified after a few years for production wells to investigate flow rate and zonal contribution of different producing layer from temperature responses in the wellbore by Curtis and Witterholt (1973). When the production rate is at least hundred barrels and the well has been producing for a long time and the overall heat transfer coefficient is high enough, the equation can be simplified by using the earth's thermal diffusivity of 33.6 Btu/day-ft-^{o}F (209328 Joules/ (m-day-^{o}C)) (Antonio, 1969)

$$A = 4.74x10^{-3} q\rho_f c_f f(t) \quad (8)$$

$$q = \frac{A}{4.74x10^{-3}\rho_f c_f f(t)} \quad (9)$$

Ramey's modified temperature model for produced fluid temperature in well bore is given below.

$$T_f(z,t) = T_{Ge} - g_G z + g_G A + \left(T_{fe} - T_{Ge} - g_G A\right)e^{-z/A} \quad (10)$$

Producing layers can be identified by changing temperature response of the flowing fluid on the temperature logs. For multilayer analysis each producing layer can be analysed individually by applying **Eq. 10** to each production layer. The amount of fluid which can create corresponding temperature response can be calculated. Since the value of *A* is proportional to the mass flow rate and production time, the distance from geothermal profile increases by mass flow rate or producing time. In **Fig.1** It can be seen that increasing mass flow rate increases the distance between the geothermal profile and the asymptote as well as the value of *f(t).*

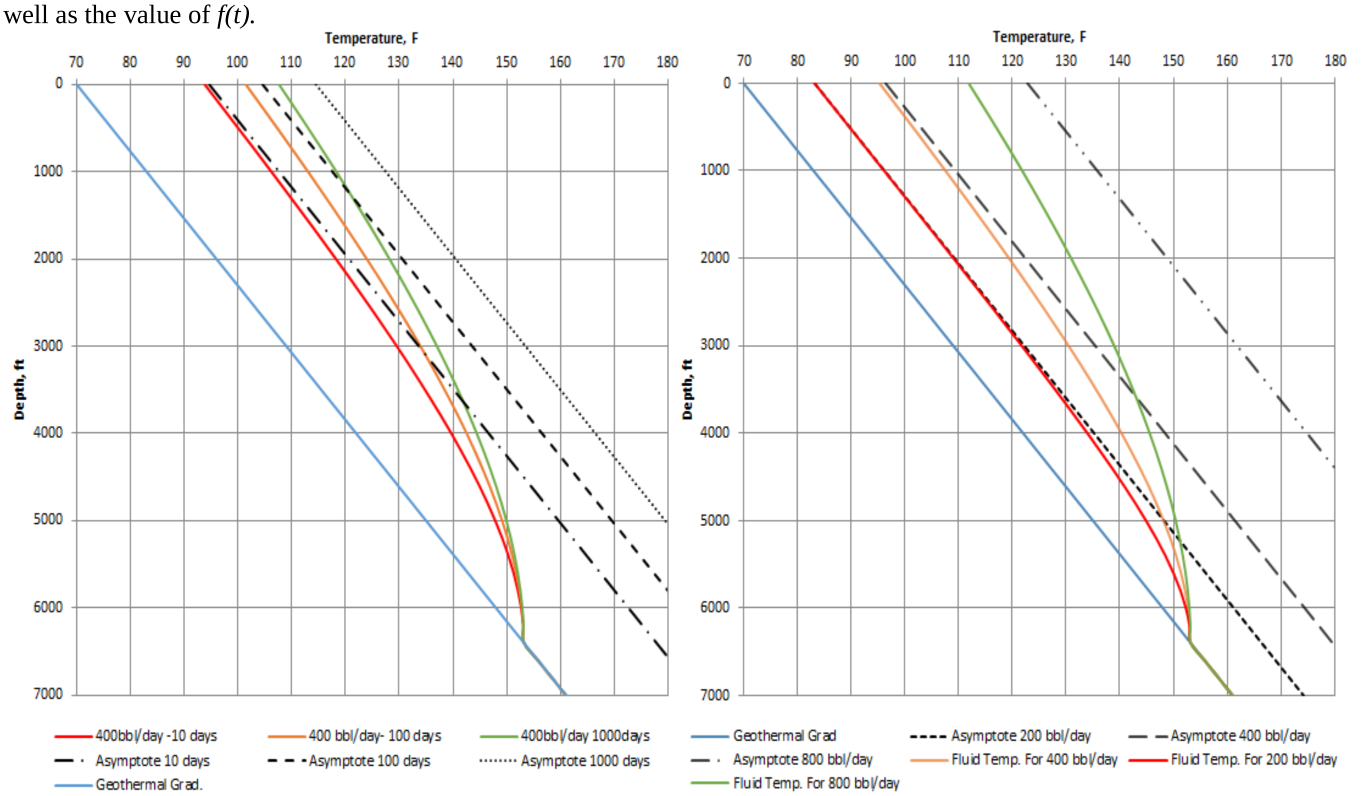

Figure 1: As production time increases, the flowing fluid temperature increases and the value of asymptote moves away from the geothermal temperature line. Also, Increasing flow rate increases the asymptote value and the displacement of asymptote is proportional to the value of flow rate.

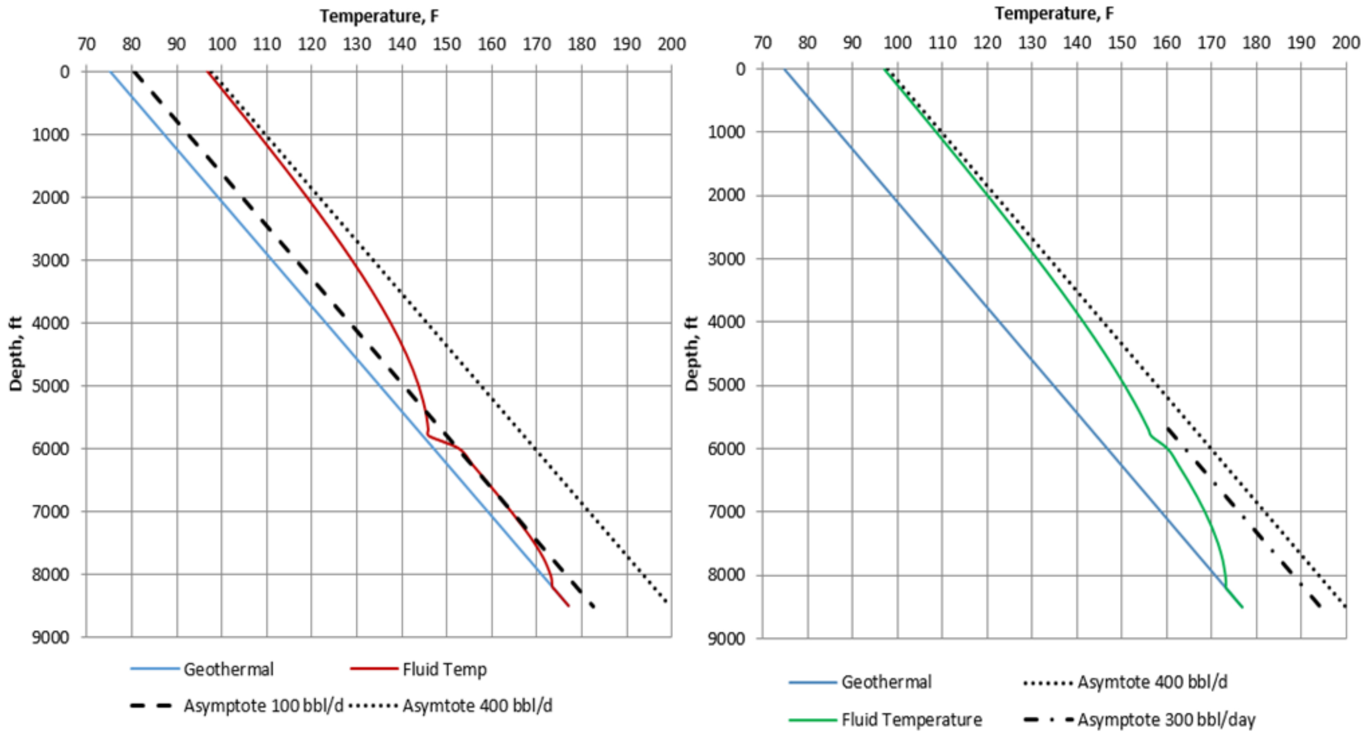

Figure 2: For both case, calculated temperature response reached corresponding asymptote after upper completion since they response the same flow rate. However, on the right hand side, fluid enters from upper completion before the temperature does not reach the asymptote due to higher flow rate (300bbl/day) comparing to the temperature response of the lower part of the left hand side.

In some cases produced fluid does not only come from one reservoir layer. The well can be completed with several layers and their contribution into total flow can be different. Therefore, the temperature response will be changed by different flows to the well bore from different layers. In the following example production comes from two different intervals with two different production rates. The first interval is between *5700-5800 ft (1737.36-1767.84 m)* and the second interval is between *8100-8200 ft (2468.9-2499.4m)* with relative flow rates *100bbl/day (15.9m^3/day)* and *300bbl/day (47.7m^3/day)*. Different temperature responses of different production rates from different production zones are represented in **Fig.2**. On the left hand side *100bbl/day (15.9m^3/day)* of oil comes from lower completion zone and *300bbl/day (47.7m^3/day)* of oil comes from the upper completion part. The temperature response of the lower part has reached its asymptote before the second produced zone then *100bbl/day (15.9m^3/day)* entry comes from upper completion.

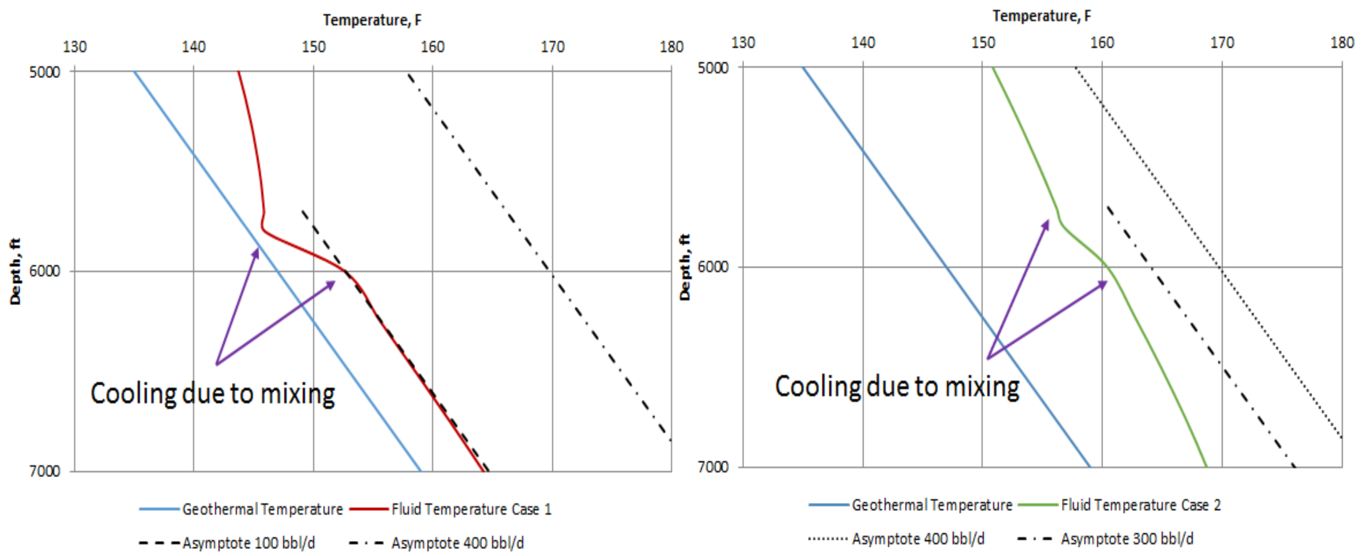

Figure 3: Expanded form of Fig.2. The amplitude of cooling is different for two cases. In the second case more hot fluids comes from lower completion and when it converges with fluids from upper zone it cools. The amount of cooling is less than in the first case due to less amount of cooler fluid entering from upper zone.

Because the temperature of the upper produced zone is cooler than of the flowing fluid the temperature curve shows a slight decrease due to fluid mixing. After the second production zone the temperature response for *400bbl/day (63.6m^3/d)* approaches its asymptote near surface. However, in the second case *300bbl/day (47.7m^3/d)* of that oil comes from lower completion and *100bbl/day (15.9m^3/d)* comes from upper completion. Because, more fluid enters from the lower zone, the temperature is higher, when it mixes with the upper fluid entry; the decrease in temperature is less than the first case **Fig.3**

As a result, the asymptote value is higher than in the case one for the lower zone due to higher fluid rate come from lower completion. Hence, second fluid enters from upper completion before the fluid from lower zone does not reach the asymptote. This case is not favourable to analyse flow rate from temperature response. Although total flow rate can be estimated by analysing the temperature response after upper completion, relative flow rates cannot be correctly estimated for the second case. However, it is possible to perform for the first case because in both temperature responses reached their asymptotes.

Calculation of flow rate from the temperature response

In **Fig.4** the temperature response shows single layer fluid entry from the depth of *11200ft (3413.8m)*. It is possible to calculate the rate of the fluid entry with the knowledge of the theory as explained above. Firstly, the geothermal temperature distribution should be created which can be easily derived from base temperature logs some days after completion to minimize the effect of cementing and before production. Without a base temperature log, temperature distribution of the deepest nonproducing section can be extrapolated upwards as a geothermal gradient. In **Fig.4** geothermal temperature is determined and extrapolated from the upper section to down and matches with the nonproducing zone measured temperature.

It is possible to find the value of the "*A"* is from the asymptote, as indicated before, the difference between geothermal profile and the asymptote is $g_G A$ then the value for A can be calculated if temperature curve is reached to asymptote and parallel to geothermal gradient. Also, Romeo-Juarez (1969) proposed a method for field calculation is valid for evaluation of the value of A.

$$A = \frac{T_{fz} - T_{Gz}}{slopeT_{fz}} \quad \text{.........} (11)$$

The flowing fluid temperature T_{fz} and geothermal temperature T_{Gz} can be read from temperature log for any given depth as well as the slope of T_{fz}. By using this method all the exponential parts of the temperature log are taken into account while calculating slope of T_{fz}. In this particular example following values are read from temperature log as flowing fluid temperature $T_{fz}=201^oF$ (93.89^oC), geothermal gradient $T_{Gz}=188.5^oF$ (86.94^oC) and the slope of T_{fz} *is* $=0.0095^oF/ft$ $(0.0173^oC/m)$. Then value of $A=1315.7ft$ *(401.12 m)* calculated from **Eq.11**.

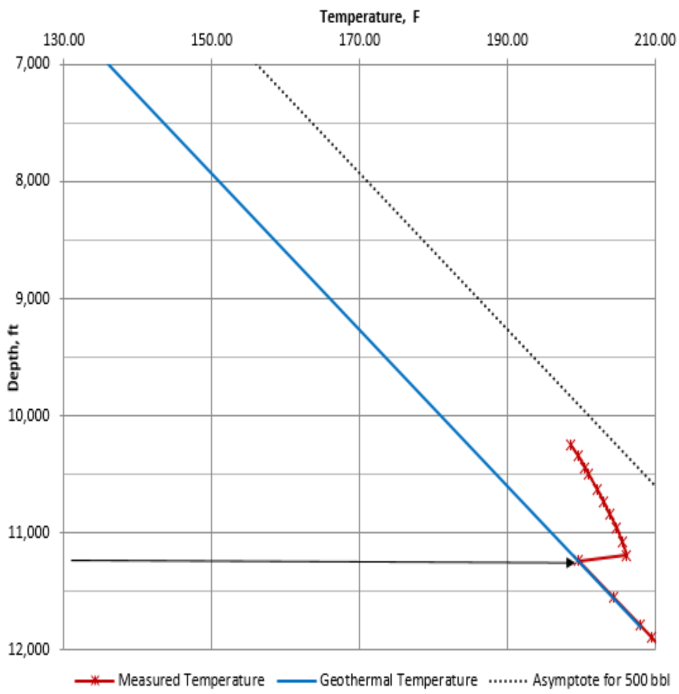

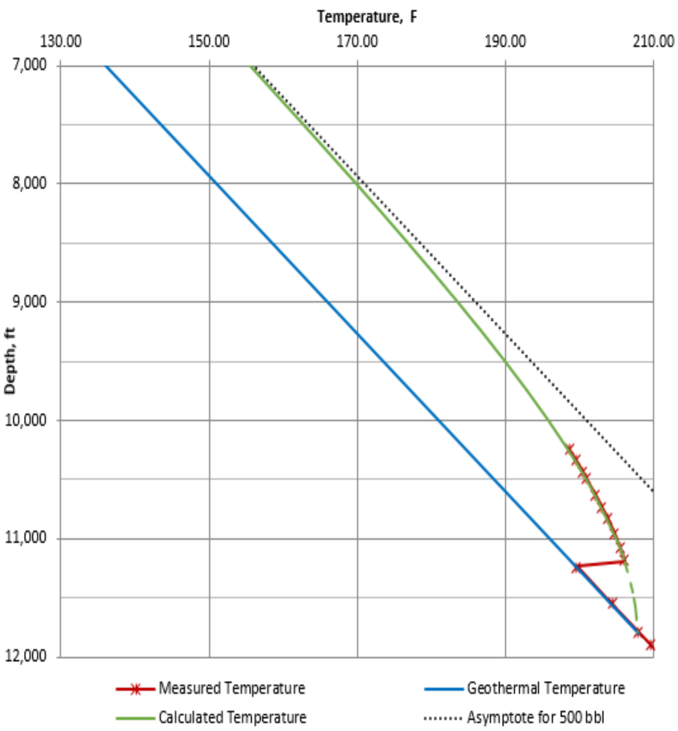

Figure 4: Calculated temperature curve is fitted to measured temperature curve by using Eq.9 and calculated the value of *A=1337.56 ft* from Eq.10 which corresponds the flow rate 500bbl/day.

After this step, fluid entry temperature and the corresponding geothermal temperature are read from the temperature log, and then these values are applied in **Eq. 10.** The temperature response of the flowing fluid is plotted and *A* value is arranged to fit it with the measured temperature curve and *A* is found *1337.56 ft(407.7m)*. Finally, the asymptote can be calculated by adding $g_G A$ to the geothermal temperature. When asymptote is plotted, calculated fluid temperature is approaching and converging with asymptote at the depth of 7500ft (2286m). Now using **Eq. 5,** with the producing time 3.7 days and thermal diffusivity of earth 0.96 ft^2/day (0.89m^2/day) and external casing radius 0.375*ft* (0.1143m) and value of *f(t)*is found 2.018. To find flow rate, **Eq. 9** is used with the value of $c_f=1\ Btu/lb\text{-}^oF$ (4186.8 J/kg-^{o}C) and $\rho_f=280\ lbm/bbl\ (800\ kg/m^3)$ and total flow rate is found *500bbl/day (79.5*m^3*/day).*

Field Examples

In this section two field examples from the Uinta basin of Utah will be analysed and the contributions of different production zones will be calculated and compared with production logging tool measurements (Curtis& Witterholt, 1972). The parameters used in analysis are listed in **Table 1**. These temperature responses illustrate the production through liner below the casing. Hence, the equations will be used in simplified form, however, for complex production strings the heat transfer mechanism must be modified. Also, during the analysis the production problem flow behind casing or liner will be represented and explained below.

	Oil Producing Well		**Oil and Water Producing Well**	
	Total Flow Rate Response		**Total Flow Rate Response**	
	Oilfield Units	**SI Units**	**Oilfield Units**	**SI Units**
Geothermal gradient, g_G	0.016 F/ft	0.0291 ^{o}C/m	0.016 F/ft	0.0291 ^{o}C/m
Fluid entry temperature, T_{fz}	219.5 ^oF	104.2 ^{o}C	213.05 ^oF	100.58 ^{o}C
Entry point geothermal temperature, T_{Ge}	213.1 ^oF	100.6 ^{o}C	201.2 ^oF	94.00 ^{o}C
Calculated value of *A*	1610 ft	490.73 m	10100 ft	5282.15 m
Depth of fluid entry, *z*	12775 ft	3893.8 m	12262.9 ft	3737.7 m
Casing outside radius	0.229 ft	0.698 m	0.208 ft	0.0634 m
Production time, t_p	62 days	62 days	20 days	62 days
Thermal diffusivity of earth, α	0.96 ft^2/day	0.089 m^2/day	0.96 ft^2/day	0.089 m^2/day
Fluid density, ρ	225.5 lb/bbl	730 kg/m^3	262.5 lb/bbl	750 kg/m^3
Specific heat capacity of fluid, c_f	1 btu/lb-^{o}F	4186.8 J/kg-^{o}C	1 btu/lb-^{o}F	4186.8 J/kg-^{o}C

Table 1: Reported and calculated parameters for the analysis of temperature distribution as a function of depth and A which is proportional to flow rate in oil producing well.

Oil Producing Well

To perform a successful temperature analysis, it is essential to know or estimate the real geothermal profile. In these examples, geothermal gradient assumed linear and extrapolated from a deeper section of the well to the surface. To get more accurate results, geothermal gradient survey should be run before the production. The reported and calculated parameters for the analysis are represented in **Table 1.**

The geothermal gradient is assumed to be $g_G=0.016\ ^oF/ft$ (0.0291 ^{o}C/m) and extrapolated from the deepest non production zone. Temperature log and spinner flow meter measurements are represented in left hand side of **Fig 5.** The temperature responds to mass flow rate with its exponential behavior. Since fluid enters wellbore, the temperature response is changed so that it is possible to figure out fluid entry points and relative amount of fluid from the amplitude of the change in the temperature response. Applying this logic, the largest amount of fluid enters from 12775ft (3893.8 m). To calculate the value of the *A*, fluid entry temperature $T_{fz}=219.5\ ^oF\ (104.2\ ^o$C) and geothermal temperature $T_{Gz}=213.1\ ^oF\ (100.6\ ^o$C) are read from the temperature log from 12700ft(3871m) because it is last apparent part of the exponential behavior. Then, using the equation above to match with the same exponent the value of *A=1610 ft (490.72m)* is found. This process cannot affect the calculation as long as it follows same exponential behavior. Subsequently, when match is achieved between calculated and measured temperature, the asymptote for total flow calculated by the distance from $g_G A$ from geothermal temperature and apparently calculated temperature profile approaches to asymptote and match after *8000 ft (2438.4m)* **(see Appendix D**).

Zone	**Flow Meter**	**Temperature Model**				
	Total Flow %	**A, ft**	**A, m**	**Flow Rate, bbl/day**	**Flow Rate, m^3/day**	**Total Flow %**
Above Zone 1	100	1610	490.73	340	54.05	100
Zone 1	70	-	-	-	-	-
Zone 2	30	605	184.40	127.7	20.3	37.5
Zone 3	-	38	11.58	7.90	1.26	2.3
Zone 4	-	42	12.8	8.86	1.4	2.4
Zone 5	-	18	5.48	3.80	0.6	1.1

Table 2: Reported rates from flow meter and calculated zonal contribution of the layers.

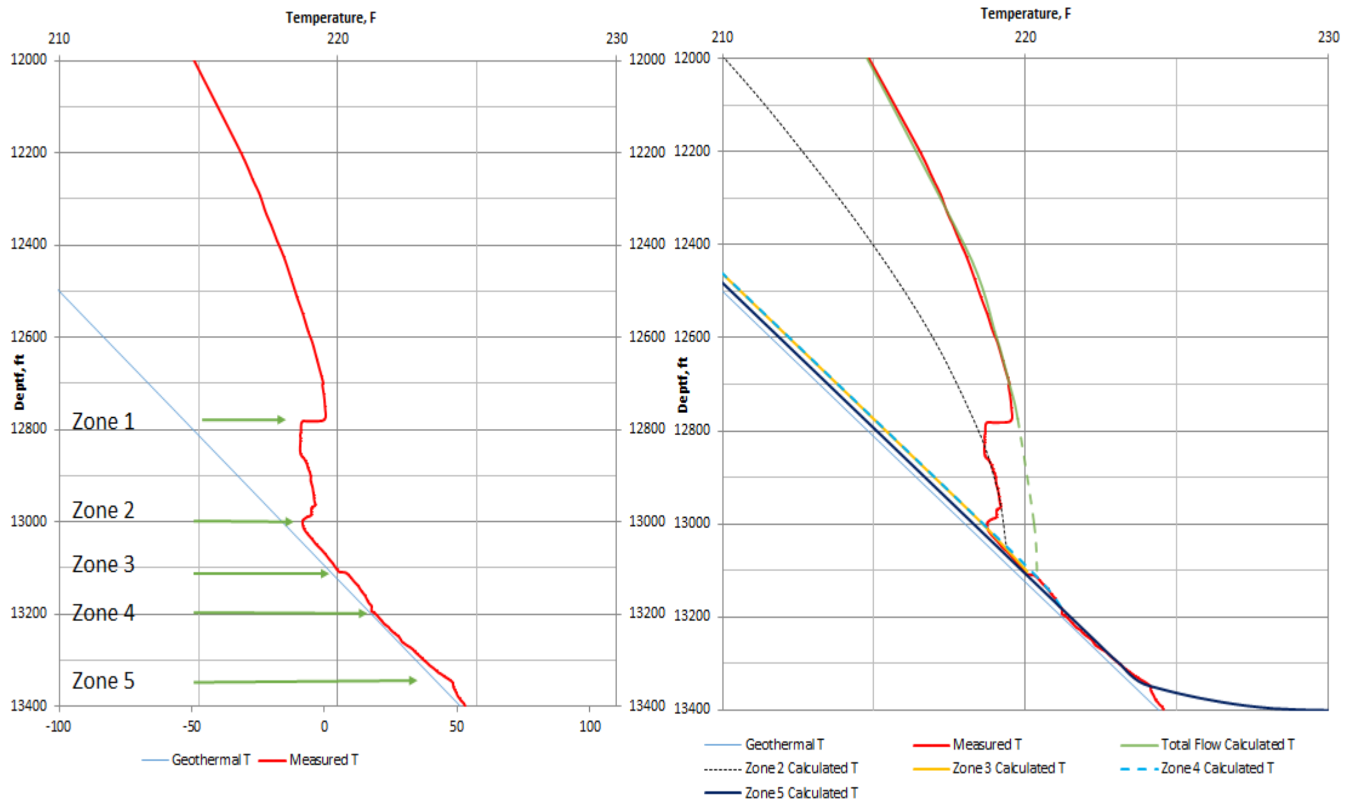

Figure 5: The measured temperature and identification of fluid entry zones are presented on the right side of the figure. Moreover, the calculated fluid temperature for each zone and the measured temperature are presented on the right side of the figure. Small portion of flow enters from zone 5 which is marginally higher than geothermal temperature hence it follows a reverse exponential behaviour afterwards and it nearly returns to the geothermal temperature behaviour. Entry from zone 4 and zone 3 are very small portion of total flow rate therefore, it cannot be detected by flow meter, however; significant flow entry can be seen on zone 2. The flow meter shows odd response at zone 2 which is due to turbulent flow. The temperature response above zone 2 represents %37 of the total flow rate comparing to flow meter shows %30 of total flow rate. In addition, after zone 1 both temperature response and flow meter represent %100 of total flow rates.

Considering the reported production time *t=62 days*, fluid density ρ_f *=255.5lb/bbl (730kg/m^3)l*, c_f *=1Btu/lbm-^{o}F* (4186.8J/kg-^{o}C) *and* r_{ci}*=0.23 ft (0.07m)*, produced fluid volume calculated using **Eq. 9,** *q= 340 bbl/day (55.48m^3/day)* is found. However, this well is reported with a production rate *q=900 bbl/day (143.08 m^3/day)*. Although, the well reported 62 days of production, real or effective production time is less due to the frequent shut-in periods for well testing. Hence, uncertainty in the production time is one reason for the difference between actual production rate and calculated production rate. However, even if production is time unknown, contribution of each zone can still be possible to calculate, because, *f(t)* is assumed the same for each zone and when flow fractions of each zone calculated *f(t)* value can be removed from the **Eq. 8.**

After the value of *A* is determined from the total flow rate temperature response, other producing zones are analysed to find their contribution to the total flow rate. The same approach has been used for this process and a reasonable match is achieved between the calculated temperature and the measured temperatures in **Fig. 5.** As a result the flow contribution from different zones compared with production logging tool compared with each other as seen in **Fig. 5** represented in **Table 2.**

The fraction of the flows rates both from production logging and temperature calculations is quite similar, **Table 2**. Because the flow contribution of zone 5, zone 4 and zone 3 is too small, flow meter cannot measure the contribution of this zone. In addition, flow meter shows a sudden change at zone 2 in **Fig. 5** this behaviour is suspected because of the turbulent flow at this level as a result of fluid comes from upper part of zone 2 through the annulus and enters to wellbore at this level. Because, produced fluid through annulus comes from upper zone is cooler, the temperature log shows a change as well and does not match with the calculated temperature at the beginning of zone 1, but then follows the same exponential behaviour in **Fig. 6**. The same phenomenon is observed at zone 2. This behaviour cannot be analysed with any other tool rather than flow profiling by temperature logs. Even though, this well has reported 183 perforations through depth *11200 ft* to *13500ft (3413-76-4114.8m)* **%95** of the total flow comes from between *12740-13000ft (3800.85-3962.4m)* where 22 perforations were located**.** In this sense, flow profiling from temperature response offers more precise information about the wellbore.

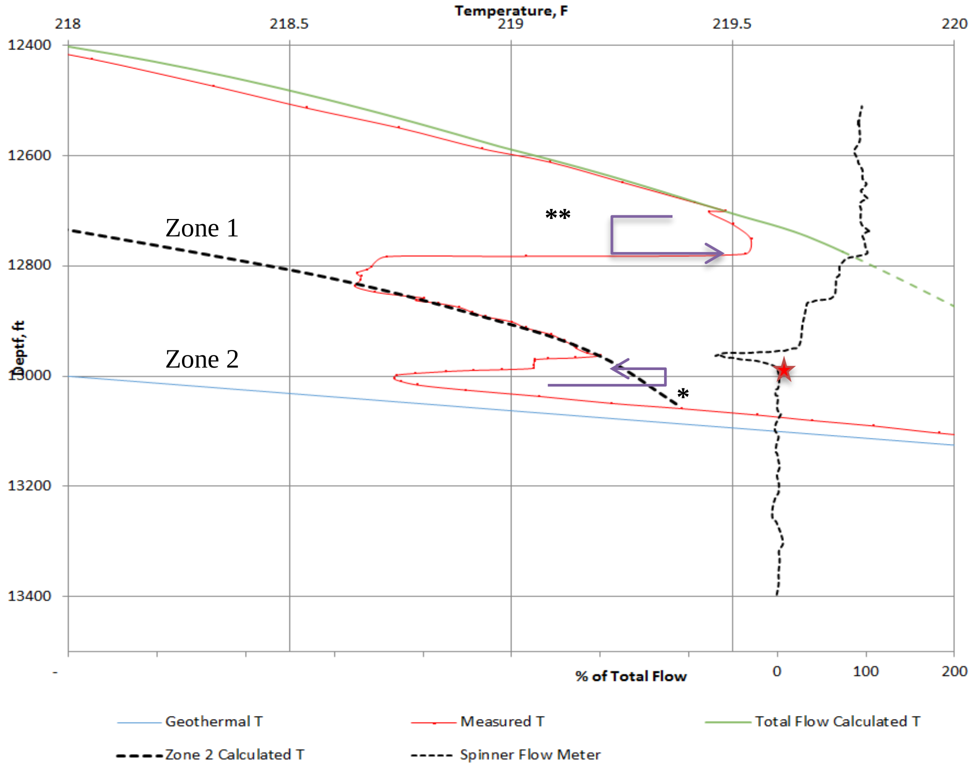

Figure 6: The production logging tool shows an abrupt change at zone two indicated by a red star. When the temperature response is investigated, flow behind casing comes from the point * and enters to wellbore at the nearest upper completion at zone 2. This phenomenon causes turbulent flow and spinner flow meter shows abrupt change. In zone 1, the measured temperature does not match with the calculated temperature at the lower part of fluid entry because; fluid comes from the point **, flows up and enters to the nearest lower perforation to the wellbore at zone 1. The fluid entering from the lower zone increases the flowing fluid temperature, conversely, the fluid entering from the upper zone decreases flowing fluid temperature.

Oil and Water Production Well

In the first example, an oil production well is analysed. However, in this section the vertical well produces water and oil together with the reported rates q_w*=700 bbl/day(111.29m^3/day)* and q_o*=1400bbl/day(222.58 m^3/day)* and no free gas at bottom hole conditions. As indicated earlier, estimating geothermal gradient is essential for a consistent analysis. The geothermal gradient is extrapolated from the lowest non-production zone to surface linearly. The reported and calculated parameters for calculation of flow rate are presented in **Table 3**. Fluid entries can be seen on temperature logs by changing temperature response and following the exponential behaviour. At the lowest producing zone there is an abrupt increase in temperature response and since it is analysed that response corresponds to a small portion of entry, this can happen in low permeability producing zones due to the friction. Also, density measurements were taken in the wellbore and it is possible to see the type of flowing fluid in the wellbore. The measurement shows that at the lowest part of the well density is around *350lb/bbl (1000kg/m^3)* which indicates water accumulation down hole. The density of the flowing fluid starts decreasing from the lowest from production until *12350 ft (3764.28m)* after which it starts to increase. This zone believed to be associated with water production.

Above Zone	Temperature Model					
	A, ft	**Zonal Contribution to Flow Rate, bbl/day f(t)=3.45**	**Total Flow Rate, bbl/day f(t)=3.45**	**Zonal Contribution to Flow Rate, bbl/day f(t)=1.735**	**Total Flow Rate, bbl/day f(t)=1.735**	**Contribution to Oil Flow Rate %**
Zone 1	10100	1634	2355	3282	4583	-
Zone 2	2681	384	721	735	1400	52.5
Zone 3	1215	306	337	593	655	43
Zone 4	166	15	31	29	62	2.1
Zone 5	90	16	16	33	33	2.3

Table 3: Contribution of each zone both corrected value of f(t) and calculated f(t).

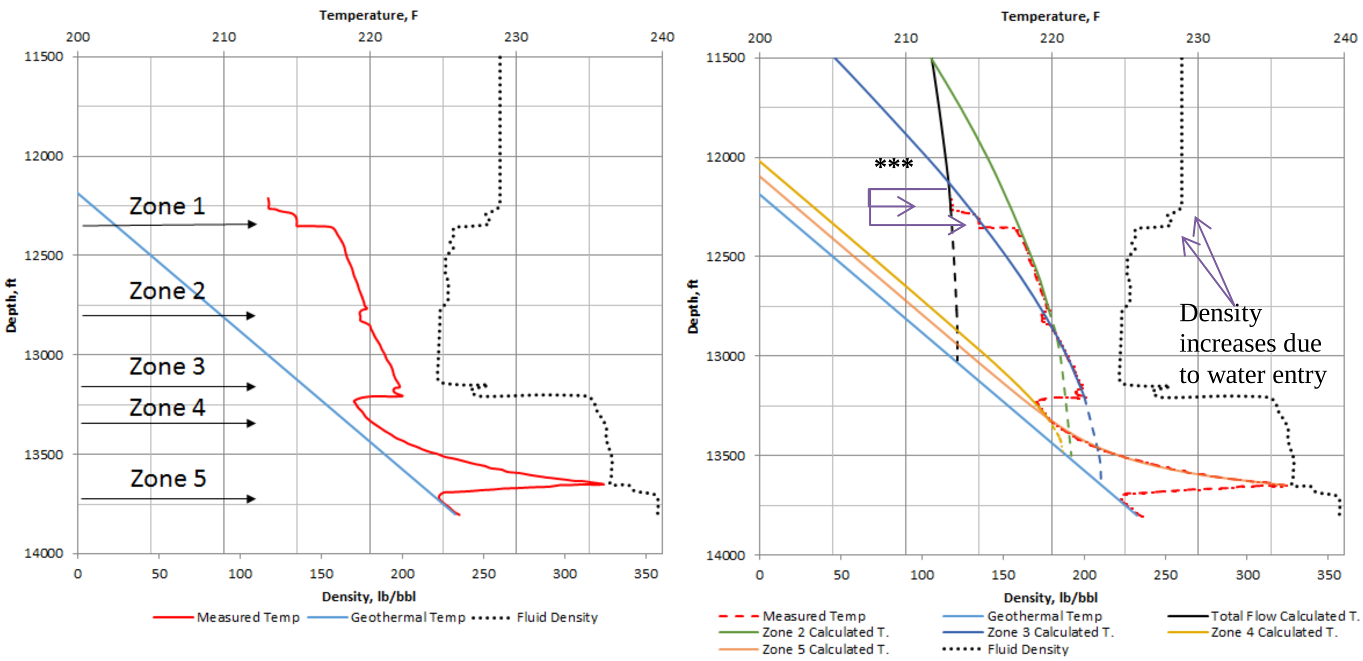

Figure 7: The calculated fluid temperature and measured fluid temperature match except for zone 1. The phenomenon of flow behind casing occurs at zone 1. Produced water comes from the point *, upper and cooler part, through the casing behind and enter the nearest perforations of zone 1. The density measurement also confirms the water entry by increasing trend on the flowing fluid density. Because, there is a cold fluid entry at zone 1, the slope of the temperature response is so high which leads to calculation of a very high value of *A*. Therefore, the calculated total flow rates are (4683bbl/day) erroneously high. As a result of the analysis, it is assumed that all oil production (1400bbl/day) comes from zone 2-3-4-5 and all water production (700bbl/day) comes from zone 1.**

In this analysis, the values for *A* are calculated by considering different production zones, fitted with **Eq. 10,** and plotted with the temperature logs show a good match with each other. Since, the well reported with 20 days of production time and r_{ci}*=0.209 ft(0.064m)*, the value of *f(t)* from **Eq. 4** becomes 3.450. Hence, total production rate calculated *2354 bbl/day* which is doubtful compared to the reported total flow rate *2100 bbl/day (333.89 m^3/day*). Also, *f(t)* value is uncertain because production time is less than 100 days. It is assumed *1400 bbl/day(222.58 m^3/day*) oil comes from lower zones, and 700 bbl/day water production comes from zone 1 which can be confirmed by density measurements because according to density measurements, the flowing fluid density increases above the depth of 12350ft (3764.28m). The flow rate is inversely proportional to dimensionless time function *f(t)* in **Eq. 9**. To calculate reported oil production rate *1400bbl/day (222.58 m^3/day)* form zone 2-3-4-5, *f(t)* value is arbitrarily change to *f(t)=1.735* to and this value of *f(t)* is assumed constant in every section of the production intervals. Although the production rates from lower zones are reasonable after *f(t)* correction, the total flow rate corresponds to the last exponential temperature response extremely high q_t*=4683bbl/day(774.53m^3/day*) comparing to the reported total flow rate q_t*=2100 bbl/day(333.89 m^3/day).*

$$A = \frac{T_{fz} - T_{Gz}}{slopeT_{fz}} = \frac{213.05 - 201.2}{0.001173} = 10100\, ft = (3078.48m)$$

$$q_t = \frac{A}{4.744x10^{-3}\rho_f c_f\, f(t)} = \frac{10100}{4.744x10^{-3}\, x262.5x1x1.735} = 4683bbl\,/\,day\left(333.89\; m^3\,/\,day\right)$$

The high total flow rate calculated is because water comes through annulus from upper and cooler part of the formation and enters at zone 1, represented in **Fig.8**, which cools the flowing fluid temperature very fast and this phenomenon decreases the slope of the flowing fluid temperature. Due to the structure of **Eq. 11**, the calculated value of *A* becomes extremely high. It can be confirmed as density measurements show an increase at zone 1 representing water entry. In addition, zone 1 has a maximum porosity value of four percent; hence, producing *700bbl/day (111.29m^3/day*) water from that zone seems impossible. Production logging tool shows an increase above these zone but not as much as *4683bbl/day (774.53m^3/day*). As a result, the total flow rate can be accepted as *2100bbl/day (333.89m^3/day)* by adding *700bbl/day (111.29m^3/day)* water production from zone 1. This well is completed with 200 perforations *12260*ft to *14470ft (3736.84-4410.45 m)* however, most of the oil production comes from zones 2-3-4-5 that have just 34 perforations.

Complex Well DTS Analysis by THERMA

Although the previous analytical model is fundamental of flow profiling using temperature data, it cannot handle complex well design and multiphase flow in the wellbore. Analysing complex data requires some complex algorithms for solution of energy, mass and momentum conservation which can be performed by thermal simulator. In this case, heat transfer in the well bore is more complex than previous case and multiphase flow is observed. The temperature response of the flowing fluid is modelled by using thermal simulator which takes into account multiphase flow, JTE and deviation of the well trajectory. The 45^o deviated well is producing from $5^{1/2}$ inch tubing and these reservoir layers are separated from each other by using swell packers. This will provide isolation of any zones in the future as required. The fiber optic cable attached to tubing with ½ inch control line provides permanent temperature monitoring along the wellbore and supply real-time data during the life time of the well. Installing fiber optic cable in the wellbore with appropriate light source becomes a high resolution temperature sensor providing measurements every meter of the distance up to twelve kilometres (Ouyang, 2005). Regarding conventional dynamic temperature logs, provided high resolution with DTS provides much precise interpretation. However, the noise level in the data can be higher sometimes so that it must be smoothed before any analysis.

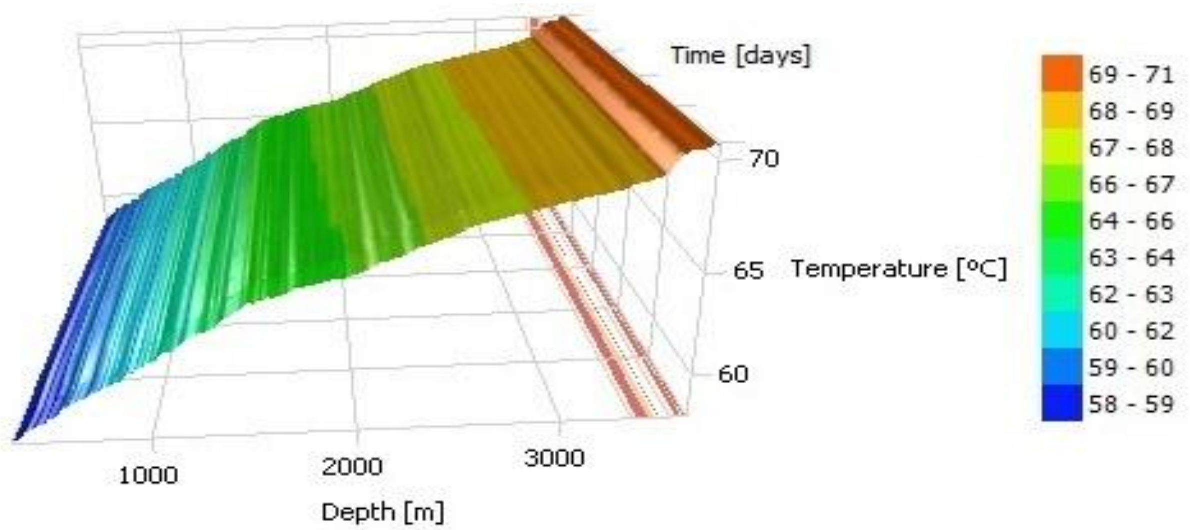

Figure8: The flowing fluid temperature distribution measured by DTS in the well bore for complex well scheme.

Schlumberger has developed THERMA, thermal modelling and analysis software which can analyse complex data using steady state approach (Brown, et al. 2007). The software takes into account multiphase flow, Joule Thomson Effect (JTE), deviation of the well and complex production string heat transfer in the energy equation and solves node by node in the wellbore.

Flow from formation to well bore occurs due to the pressure difference. This pressure difference can cause a change on flowing fluid temperature because of JTE. Contrary to previous model, THERMA can model the near wellbore region and accounts for the JTE which is a function of fluid properties, pressure change and temperature change (Brown et al. 2007). The JTE can cause cooling while flowing fluid is gas and cause heating while flowing fluid oil and water. THERMA model analyses the data taking into account frictional, elevation and internal pressure changes, and enthalpy and entropy conservation during the process of heat transfer between fluid and surroundings with calculating flow contributions from Darcy's Law in **Eq. 11** (Pinzon et al. 2010).

Reservoir Description

This reservoir consists of the three main producing unconsolidated sandstone layers with inter-bedded shale layers existing in place between each reservoir layer so that they are analysed individually and their contribution to flow rate is calculated. Distribution zones into formation and reservoir parameters are represented in **Table 3.** There is no water production and no free gas at bottom-hole conditions, however, gas oil ratio (GOR) is reported 850 SCF/STB at surface conditions. Hence, the calculation in THERMA takes in to account multiphase flow.

	Reservoir A			Reservoir B		Reservoir C		
	Zone 1	Zone 2	Zone 3	Zone 4	Zone 5	Zone6	Zone 7	Zone 8
Thickness, m	9.41	39	20.2	4.68	7.9	17.94	4.8	12.9
Permeability, md	124	124	124	50	50	442	442	442
Pressure, psi	4801.5	4836.6	4868.2	4896.3	4935.8	4969.7	4981.5	4990.8

Table 4: Measured reservoir parameters.

Analysis Process

After DTS was installed to well bore, measurement has been taken continuously throughout well bore and it is possible to observe any change in temperature response during production process. **Fig. 8** shows the temperature distribution in the wellbore at different times. Also, in **Fig. 9** temperature distribution of reservoir interval is presented. Pronounced temperature changes can be seen at production intervals and at the locations where swell packers have been placed. Since there is an additional tool in production string, due to the heat exchange, temperature response can show rapid changes which can be used to check the depth of the equipment.

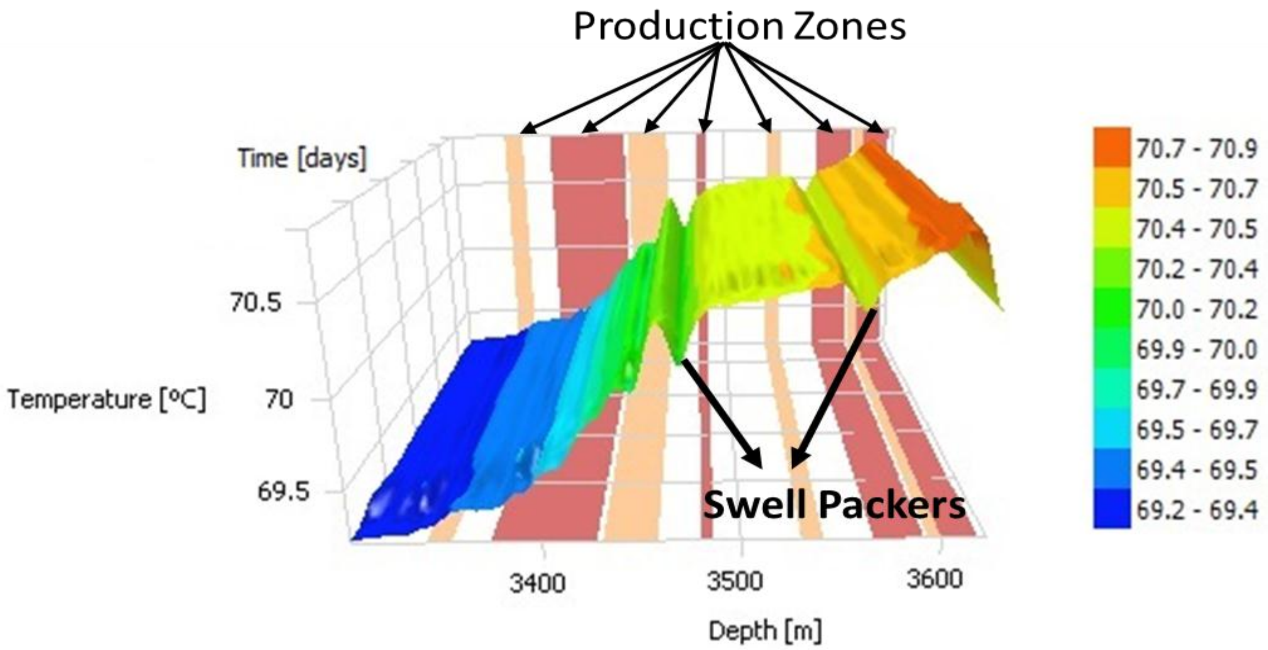

Figure 9: Production zone temperature distribution measured by DTS in wellbore.

To begin temperature analysis the geothermal gradient is assumed 2.2 ^{o}C/100m which is confirmed by near exploration wells. In the analysis layer permeability is transformed from measured while drilling (MWD) porosity logs to core permeability (Brown, et al. 2005). After, estimated layer permeability and pressures are input into the THERMA. Then THERMA models the temperature response of the flowing fluid. Since GR log imported in the graph approves the selected producing zones. The measured temperature with DTS and calculated temperature response nearly overlap each other in **Fig.10** and as expected highest contribution of the flow comes from zone 6-7-8 which have higher kh values. Contributions of all zones are listed in the **Table 5**.

Res. Layer	Zone No.	Estimated Permeability					Calculated Best Fit Permeability					
		Surface					Surface					
		Oil Rate %	Oil Rate Sm^3/day	Oil Rate STB/day	Gas Rate MMSCF /day	Gas Rate Msm^3 /day	k md	Oil Rate %	Oil Rate Sm^3/day	Oil Rate STB/d	Gas Rate MMSCF /day	Gas Rate Msm^3 /day
A	**Zone1**	4.54	102.8	646.6	0.55	15.56	90	3.11	71.75	451.3	0.38	10.86
	Zone2	18.88	427.5	2689	2.29	64.72	100	14.37	331.37	2084.3	1.77	50.17
	Zone3	9.89	223.81	1408	1.20	33.88	200	15.04	346.93	2182.2	1.85	52.52
B	**Zone4**	0.92	20.763	130.5	0.11	3.14	97	1.68	38.71	243.5	0.21	5.87
	Zone5	1.59	36.06	226.8	0.19	5.46	30	0.90	20.8	130.8	0.11	3.15
C	**Zone6**	32.71	740.64	4658.5	3.96	112.13	380	26.55	612.2	3850.5	3.27	92.7
	Zone7	8.84	200.15	1258.9	1.07	30.30	470	8.88	204.67	1287.3	1.09	30.98
	Zone8	22.63	512.22	3222	2.74	77.55	610	29.47	679.566	4274.4	3.63	102.88

Table 5: Zonal contributions of the producing zones before and after permeability optimization.

Since, the layers permeability is estimated from MWD porosity, these permeability values can be misleading and can change zone by zone. In **Eq. 12** the flow rate is function of permeability, and the temperature is function of flow rate. Therefore, when permeability is changed, the temperature response will be changed. THERMA offers a fitting algorithm for calculated temperature to match with measured DTS data by changing selected parameters. Hence, permeability was chosen as a variable and an optimization is performed on permeability. After the optimization, calculated temperature profile shows a good match with DTS measurements except the place where swell packers are located in **Fig. 11** however, this does not affect calculations. Finally, zonal flow contributions of each zone are calculated and listed in **Table 5** after individual permeability of each zone optimized.

$$q_t = \frac{7.08x10^{-3} kh\left(P_r - P_w\right)}{\mu_o B_o \left[ln\left(\frac{r_e}{r_w}\right) - 0.75 + S_t \right]} \qquad (12)$$

The correlation employs **Eq. 12** (Darcy's Law) for vertical and deviated wells and the Joshi equation for horizontal wells. The flow rate is a function of the pressure difference between formation and wellbore, permeability, reservoir thickness and skin. Therefore, when permeability is changed, flow rate will be changed proportionally and as a result temperature response of the flowing fluid will be changed. In the optimization process, individual layer permeability is changed to match with the temperature response and each layer assigned with individual permeability in **Table 6**. After the optimization simulated temperature shows better match with the measured DTS temperature and represented in **Fig. 11**. As a result, contribution of each zone is optimized and contributions of each zone are slightly changed and listed in **Table 6**.

The analysis of the temperature response shows that the highest 65% of the total flow rate is produced from the reservoir layer C, 2.5% from the reservoir layer B and 32.5% from reservoir layer C. Since the well bore pressure is high there is no free gas in the production zone. However, while pressure decreases in the upward direction, solution gas come free through wellbore. Therefore, the displayed flow rates on the **Fig. 10** and **Fig. 11** are down-hole rates. When fluids reach to the surface the solution gas becomes free due to pressure difference and oil sink and flow rate decreases at wellbore. Down-hole and surface flowing rates are calculated for gas and oil and listed in **Table 5.**

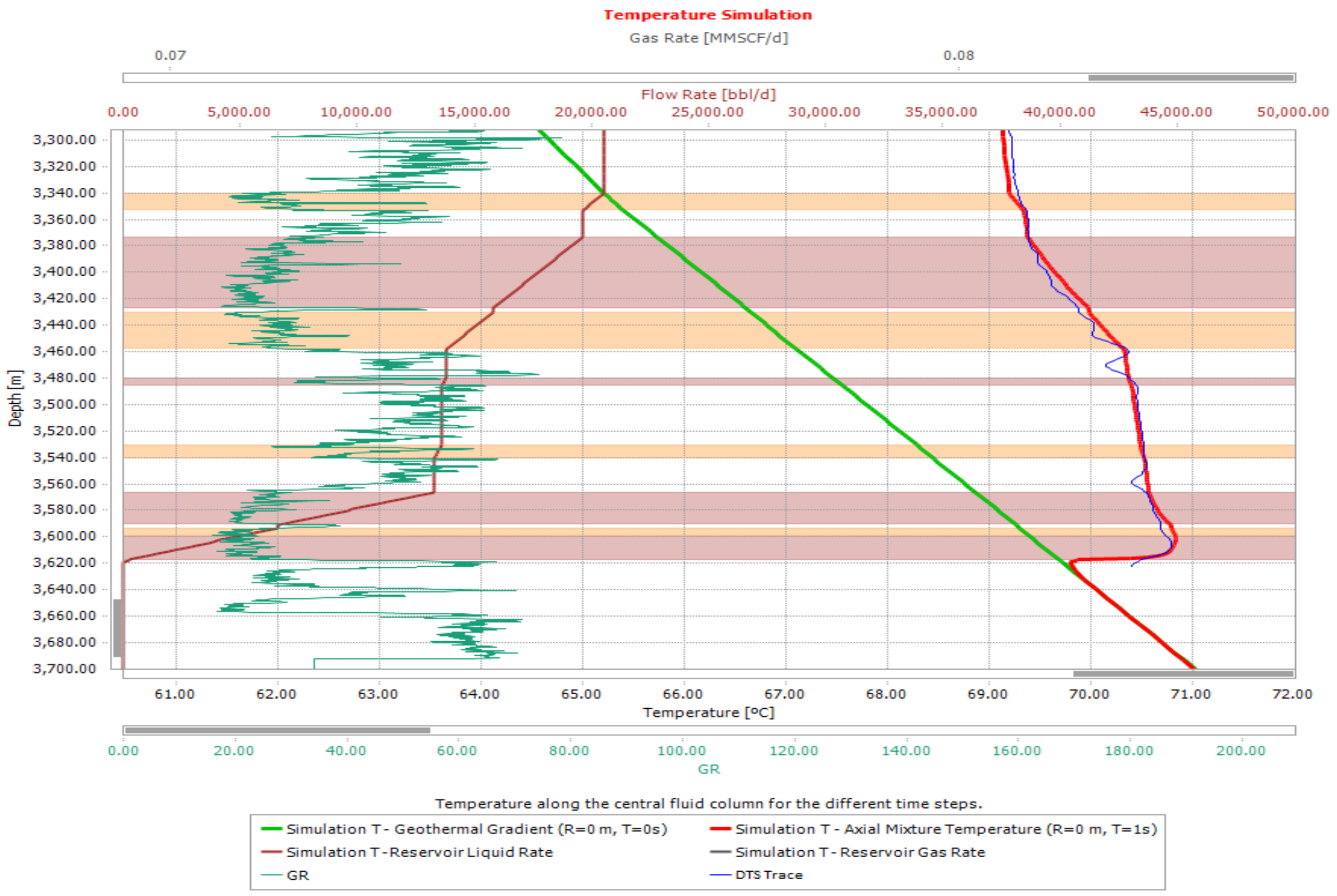

Figure 10: Selected production zones shows consistency with GR measurements and calculated temperature shows reasonable match with measured DTS data except where swell packers are located. Also, zonal contribution of the producing layers can be seen on the flow profile. Therefore, the contribution of zone C is higher than zone B and A.

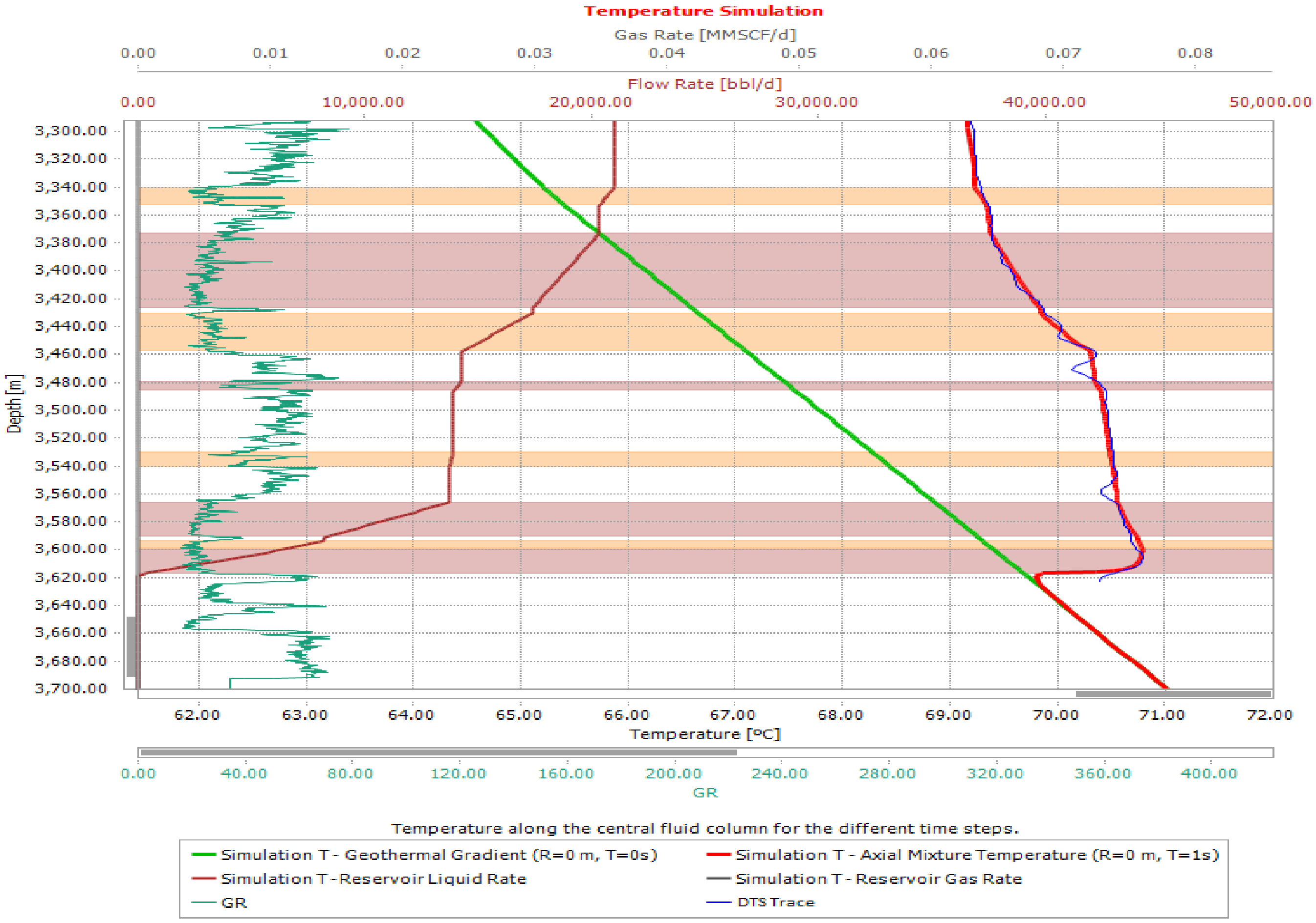

Figure 11: Flow rate is a function of permeability and temperature response is a function of flow rate. Therefore, individual layer permeability is optimised to match with DTS measured temperature. As a result, contribution of each layer is changed however, contribution of reservoir A, B and C still remained same.

Discussion

1. The main uncertainty in the analytical approach is the transient conduction heat function *f(t)*. This function has a large uncertainty in early time of production, because the temperature response has not stabilized yet. A production time of more than 100 days is necessary to represent temperature response of the well and offer an accurate solution for flow rate calculations.
2. The first analytical approach works for a single phase fluid which is assumed to be incompressible, allowing the kinetic energy and flowing friction effects to be ignored; in some cases these can be important. In addition, the proposed model is valid only for production through casing in vertical wells. Since the heat transfer coefficient of casing is significantly higher than any other material in the system, **Eq.7** can be simplified. However, it might fail for a complex well scheme.
3. The first analytical approach suggests that the flowing fluid temperature should converge with the asymptote then flow fractions can be calculated. To implement this logic, at least one hundred feet is required between two layers to reach corresponding asymptote. Otherwise, the calculated fractions can be misleading.
4. Defining the correct geothermal temperature is extremely important to calculate heat transfer between flowing fluid and surroundings and flow rate. It can be assumed constant and extrapolated linearly from deepest non production zone of formation to surface; however, this can be misleading. To solve this uncertainty, a base temperature log must be taken before production or during the shut-in period.
5. The produced fluid flows into well bore due to pressure difference between wellbore and formation. This phenomenon employs Darcy's Law which is a function of permeability. Hence, the permeability of the produced zone affects the flow rate and subsequently affects the temperature response. Having the real permeability data helps for reasonable analysis in THERMA.
6. Reservoir pressure depletes by the time of production and hence updated pressure distribution of the wellbore and formation can help to understand production layer depletion. Moreover, this information can be used to prevent cross flow between the reservoir layers.

Conclusions

Heat exchange, between the produced hot fluid and the surrounded cooler formation along the wellbore, is used to find an expression for flowing fluid temperature in the wellbore. Since the flowing fluid temperature is a function of mass flow rate, the mass flow rate is calculated from the temperature response of flowing fluid measured by the dynamic temperature logs or DTS. The analytical model developed for single phase flow by Ramey (1962) was used to analyse the first two field cases to investigate the individual layer contributions from changing temperature response. It was found that ~90% of the total flow was coming from ~15% of the perforated intervals. In addition, the contributions of non–significant producing layers and flow behind casing were detected by the temperature analysis. The results were found to be comparable with the production logging tool measurements.

Modern wells are mostly deviated or horizontal and multiphase flow regime is very common. Ramey's model is not able to calculate flow rate from the temperature response of the complex well scheme because of the multiphase flow and the deviation of the well. To calculate contribution of different reservoir layers in an example field study, the software THERMA was deployed. The software modifies the general energy equation by taking into account multiphase flow, deviation of the well and near wellbore effects. Therefore, more accurate results were obtained by using DTS data for 45^o deviated modern well. As a result, the temperature analysis of the well shows that the reservoir layer C contributes 65% of total flow, reservoir layer B contribute 2.5% and layer A contributes 32.5% of total flow. If a shut-in survey is planned in future, the temperature response should be investigated by DTS. This process can confirm if there is a cross flow in the wellbore since temperature measurements are taken continuously.

Nomenclature

		Field Units	SI Units
A	= relaxation distance parameter,	ft	m
B_o	= oil formation volume factor,	bbl/stb	m^3/sm^3
c_f	= heat capacity of fluid,	Btu/(lbm-^{o}F)	J/Kg-^{o}C
E	= internal energy	Btu/lbm	J
$f(t)$	= heat conduction time function, dimensionless	-	-
g	= acceleration owing to gravity,	ft/sec^2	m/sec^2
g_c	= conversion factor,	32.17 (lbm-ft)/(lbf-sec^2)	9.806 kgm-m/(kgf- sec^2)
g_G	= geothermal gradient,	^{o}F/ft	^{o}C/m
H	= entalphy,	Btu/lbm	J/kg
J	= mechanical equivalent of heat,	778 lbf-ft/Btu	9.80 kgf-m/J
K	= conductivity of formation	Btu/ (F-day-ft)	J/ ^{o}C-day-m
k	= permeability,	md	m^2
k_c	= conductivity of casing material,	Btu/(^{o}F-day-ft)	J/ ^{o}C-day-m
p	= absolute pressure,	psi	kgf/m^2
P_r	= reservoir pressure,	psi	kgf/m^2
P_w	= wellbore pressure,	psi	kgf/m^2
Q	= heat transfer rate per unit length of wellbore,	Btu/(day-ft)	J/(day-m)
Q_t	= heat transferred from surroundings,	Btu/lbm	J/kgm
q	= heat transfer rate,	Btu/day	J/day
q_o	= oil flow rate,	bbl/day	m^3/day
q_t	= total fluid flow rate,	bbl/day	m^3/day
q_w	= water flow rate,	bbl/day	m^3/day
r_{ci}	= casing inside radius,	ft	m
S	= skin,	-	-
t	= production time,	day	day
T_0	= injection fluid temperature,	^{o}F	^{o}C
T_e	= formation temperature,	^{o}F	^{o}C
T_f	= flowing fluid temperature,	^{o}F	^{o}C
T_{fe}	= fluid entry temperature to wellbore,	^{o}F	^{o}C
T_{Ge}	= geothermal temperature,	^{o}F	^{o}C
T_{Gs}	= surface geothermal temperature,	^{o}F	^{o}C
u	= fluid velocity,	ft/sec	m/sec
U	= overall heat transfer coefficient,	Btu/(day-ft^2- ^{o}F)	J/(day-m^2 ^{o}C)
V	= specific volume,	bbl	m^3
W	= fluid mass rate,	lbm/day	kgm/day
W_f	= flow work,	ft-lbf/lbm	kgf-m/kgm
z	= distance from production or injection point,	ft	m
α	= heat diffusivity of earth,	ft^2/day	m^2/day

ρ_f	= flowing fluid density,	lb/bbl	kg/m3
μ	= fluid viscosity	cp	kg/(m-s)

References

[1] Antonio, J. R., "A note on the theory of temperature logging", SPE -2464. SPE Journal Vol.9, December 1969, 375-377.

[2] Brown, G. A., Greenaway, R., Carney, M., Meyer, J. H., Davies, E. J., Prizion, D.I. "Permanent monitoring: Taking it to reservoir", Oilfield Review Spring, Vol.22, (2010) 34-41

[3] Brown, G.A., Field, D., Davies, J., Collins, P., Garayeva, N. "Production monitoring through openhole gravel-pack completions using permanently installed fiber-optic distributed temperature systems in BP-Operated Azeri Filed in Azerbaijan", SPE-95419, proceedings of the SPE Annual Technical Conference and Exhibition, Texas, USA, October 2005.

[4] Curtis, M.R., Witterholt, E. J. "Use of temperature log for determining flow rates in producing wells", SPE -4637-MS proceedings of the SPE 48th Annual Technical Conference and Exhibition, Las Vegas, Nevada, October 1973.

[5] Hasan, A. R., Kabir, C. S. "Fluid and heat transfer in wellbores". Texas: Society of Petroleum Engineers. 2002, 64-70.

[6] Hasan, A. R., Kabir, C. S., Wang, X. "A robust steady-state model for flowing fluid temperature in complex wells". SPE -109765, proceedings of the SPE Annual Technical Conference and Exhibition, Anaheim, California, November 2007.

[7] Nowak, T. J. "Estimation of water injection profiles from temperature surveys", SPE 953203, Journal of Petroleum Technology, Vol. 5, August 1953, 203-212.

[8] Ouyang, L. B. "Production and injection profiling- challenges and new opportunities" SPE-2005, proceedings of the 46th Annual Logging Symposium, New Orleans, California, June 2005.

[9] Pinzon, I.D., Davies, J.E., Mammadkhan, F., Brown, G.A. "Monitoring production from gravel-packed sand-screen completions on BP`s Azeri Field using permanently 'installed distributed temperature sensors". SPE-110064, proceedings of the SPE Annual Technical Conference and Exhibition, California, USA, November 2007.

[10] Ramey, H.J. "Wellbore Heat Transmission", SPE-96 Journal of Petroleum Technology, April 1962, 427-435.

[11] Schlumberger, M., Doll, H. G., Perebinossoff, A. A., "Temperature measurements in oil wells": Institute of Petroleum Technologists Journal, Vol.23, London, 1937, 1-25.

APPENDIX A
Critical Literature Review

Milestones				
SPE Paper n°	**Year**	**Title**	**Authors**	**Contribution**
953203	1953	"The Estimation of Water Injection Profiles From Temperature Surveys"	Nowak, T. J.	Very first paper describes a quantitive approach to flow allocation.
96	1962	" Wellbore Heat Transmission"	Ramey, H. J.	First paper presents approximate solution to the wellbore temperature predicting model.
4637	1973	"Use Of The Temperature Log For Determining Flow Rates In Producing Wells"	Curtis, M.R., Witterholt, E.J.	Use of energy equation in to practice. Illustrate the use of dynamic temperature logs to determine flow rate. Also some production problems pointed by using temperature logs.
19702	1991	Predicting temperature profiles in a flowing well.	Sagar, R. Doty, D. R. Schmidt, Z.	Extendend version of Ramey's model for multiphase flow and accounting the Joule Thomson Effect in the model. This model then simplified for engineering calculations however, simplified model sometimes cannot be successful.
2005	2005	"Production and Injection Profiling Challenges and New Opportunities"	Ouyang, L.B.	Clear explanations for the new technologies applied on production profiling by using DTS and PDG.
95419	2005	"Production Monitoring Through Open Hole Gravel-Pack Completions Using Permanently Installed Fiber-Optic Distributed Temperature Systems in the BP-Operated Azeri Field in Azerbaijan"	G. Brown, J. Davies, N. Garayeva,	This study uses DTS temperature data and the software THERMA developed by Schlumberger in open-hole gravel pack completion to analyze flow profile.
92962	2005	"Monitoring of real-time temperature profiles across multi zone reservoirs during production and shut-in periods using permanent fiber-optic distributed temperature systems."	Frayer, V., Shuxing, D., Otsubo, Y., Brown, G., Guilfoyle, P.	Explain how DTS system can be used to determine temperature profiles and compares temperature distribution for different flow rates. This will help to understand how temperature profile is changing by flow rate.
109765	2007	"A robust Steady-State Model for Flowing-Fluid Temperature in Complex Wells"	A.R. Hasan, C.S. Kabir, X. Wang	Present a new approach for an analytical model for wellbore flowing fluid temperature with changing wellbore trajectory and thermal properties of the well surroundings.
111790	2008	"Modeling flow profile using distributed temperature sensors (DTS) system"	Wang, X., Lee, J., Vachon, G.	This model is modified form of robust model of Hasan and Kabir for different production zones. It provides good approximation for estimating flow profile from different zones.
120805	2008	Distributed temperature system (DTS) modelling and applications.	Wang, X., Lee, J., Vachon, G.	This model is modified form of robust model of Hasan and Kabir for different production zones. It provides good approximation for estimating flow profile from different zones. In addition, model demonstrates the gas lift points injection profiles.

APPENDIX B
SPE-953203 (1953)

The Estimation of Water Injection Profiles From Temperature Surveys

Authors: Nowak, T. J.

Contribution to the understanding of analysis of temperature response to determine flow rates in producing zones:
First non-robust model applied to profile injectivity by using heat transfer phenomena.

Objective of the paper:
Determine water intake profile on different strata in wellbore.

Methodology used:
Temperature distribution is assumed instant and function of time in infinite radius solid cylinder. Temperature distribution in the wellbore obtained considering linear sink of heat on the formation.

$$(T_o - T_w) = \Delta T_2 = \frac{Q_{1-2}}{4\pi K} ln \frac{\theta_3 - \theta_2}{\theta_3 - \theta_1}$$

T_o = Formation temperature at unit depth.
T_w = Average temperature in the wellbore.
$Q_{1,2}$ = Heat transfer rate per unit depth
Θ_1 = Initial time of water injection =0
Θ_2 = Total time from beginning to end of the injection
Θ_3 = Total time from beginning of the injection history to particular time of shut-in.

Conclusion reached:
Injectivity profiles estimated using heat transfer phenomena. Although, poor resolution of the estimation regarding PLT measurements, it estimates the layers can intake the injected fluid.

Comments:

SPE-953203 (1962)

Wellbore Heat Transmission

<u>Authors</u>: Ramey, H. J.

<u>Contribution to the understanding of analysis of temperature response to determine flow rates in producing zones:</u>
First pioneering model for defining wellbore heat transmission for injection wells. The model is still valid in application for specific wells. Most of the recent models are depended on the model created by Ramey.

<u>Objective of the paper:</u>
The heat transfer model was pronounced to model injection profiles for single phase fluids by solving energy conversation equation.

<u>Methodology used:</u>
Energy equation is solved to define flowing fluid temperature for injection wells under steady state conditions and expression is derived for flowing fluid as follows.

$$T_f\left(\mathrm{z},t\right)=T_{GS}+g_G z-g_G A+\left[T_0\left(t\right)+g_G A-T_{GS}\right]e^{-z/A}$$

<u>Conclusion reached:</u>
A formulation for flowing fluid temperature is defined and from this approach injection profile can be built using dynamic temperature logs. Successful applications were explained in the paper. Most importantly, this model is valid for some cases, and most of robust models are still referencing Ramey’s model.

<u>Comments:</u>
Friction and kinetic energy terms are ignored to approximate the solution however, for complex well schematics and multiphase flow this model does not work. It carries uncertainty for early times of injection.

SPE-4637 (1973)

Use of Temperature Log For Determining Flow Rates In Producing Wells

Authors: Curtis, M.R., Witterholt, E.J

Contribution to the understanding of analysis of temperature response to determine flow rates in producing zones:
First application of determining contribution of different producing zones into total flow. Valid under steady state conditions and under some assumptions.

Objective of the paper:
Temperature behavior of produced fluid is explained and fraction of different production zones are calculated from field examples.

Methodology used:
This study modified the model proposed by Ramey[3] for production wells. The modified temperature expression for producing wells

$$T_f\left(z,t\right)=T_{Ge}-g_G z+g_G A+\left(T_{fe}-T_{Ge}-g_G A\right)e^{-z/A}$$

Conclusion reached:
Contributions of different producing layers are calculated using modified form of Ramey and confirmed by other production logging tools.

Comments:
Model is still valid for not complex production wells. Interpretations can be misleading with the temperature response less than one hundred days.

SPE-19702 (1991)

Predicting temperature profiles in a flowing well

Authors: Sagar, R., Doty, D. R., Schmidt, Z

Contribution to the understanding of analysis of temperature response to determine flow rates in producing zones:
Extended version of Ramey's model[3] for multiphase flow and accounting the Joule Thomson Effect in the model.

Objective of the paper:
Calculation of temperature response of producing wells by using two models which are steady state heat transfer and simplified version of the first model for hand calculation.

Methodology used:
The model is pretty much same with the model proposed by Ramey[3], however, Joule Thomson Effect is adopted and ignored kinetic energy part of energy equation is used in this model.

Conclusion reached:
Wellbore temperature calculated by using offered models. The models shows good agreement, however, there is 2.4 ^{o}F absolute error between these two models when flow rate is greater than 5lb/sec. Otherwise, 3.9 ^{o}F.

Comments:
The model does not take into account for convectional heat transfer in wellbore. Litreture review shows that temperature response without convectional calculations can be higher than real profile.

SPE-2005

Production and Injection Profiling Challenges and New Opportunities

Authors: Ouyang, L.B.

Contribution to the understanding of analysis of temperature response to determine flow rates in producing zones:
Clear explanations for the new technologies applied on production profiling by using DTS and PDG.

Objective of the paper:
This paper represents the challenges on flow profiling by using DTS measurements. Also discussed the method proposed by same authors on both field and simulated data.

Methodology used:
Temperature estimation is performed using mass, momentum and energy balance by discretization of wellbore.

$$\begin{aligned}(\rho_o q_o h_o + \rho_g q_g h_g + \rho_w q_w h_w)_{j+1} - \left(\rho_o q_o h_o + \rho_g q_g h_g + \rho_w q_w h_w\right)_j \\ = -2\pi r_w \Delta z\left(\rho_{eo} V_{eo} h_{fo} + \rho_{ew} V_{ew} h_{fw}\right)_j + 2\pi r_w U \Delta z (T_w - T_r)_j\end{aligned}$$

$$V_{ei,j} = \frac{\rho_{ij+1} q_{ij+1} - \rho_{ij} q_{ij}}{2\pi r_w \Delta z q_{eij}}$$

Conclusion reached:

The model is good at temperature profiling when known rates are applied. Although, it can fails to estimate flow profile under multiphase flow, it can successfully estimate single phase flow profiling.

Comments:

SPE-95419 (2005)

Production Monitoring Through Open-hole Gravel-Pack Completions Using Permanently Installed Fiber-Optic Distributed Temperature Systems in the BP-Operated Azeri Field in Azerbaijan

Authors: Brown, G. A., Davies, J., Garayeva, A.

Contribution to the understanding of analysis of temperature response to determine flow rates in producing zones:
This study uses DTS temperature data and the software THERMA developed by Schlumberger in open-hole gravel pack completion to analyze flow profile.

Objective of the paper:
The main objective of the paper is calculate zonal contribution of different zones and evaluation of the reservoir during production time.

Methodology used:
The motivation behind the this thermal modelling software is using steady state pressure model together with a transient thermal solution that can model most black oil scenarios to facilitate analysis of DTS temperature data

Conclusion reached:
Contributions of different layers (gas and oil rates) are precisely calculated. The permeability of each zone which is converted from porosity log to core permeability, is optimized regarding temperature data. Finally, most production zone is determined and future reservoir surveillance will be done regarding this analysis.

Comments:
The software has been tested and provides very good solution for both single phase and multiphase flow.

SPE-92962 (2005)

Monitoring of real-time temperature profiles across multi zone reservoirs during production and shut-in periods using permanent fiber-optic distributed temperature systems.

Authors: Frayer, V., Shuxing, D., Otsubo, Y., Brown, G., Guilfoyle, P.

Contribution to the understanding of analysis of temperature response to determine flow rates in producing zones:
This paper explains how DTS system can be used to determine temperature profiles and compares temperature distribution for different flow rates. This will help to understand how temperature profile is changing by flow rate.

Objective of the paper:
The objective is to monitor and evaluate reservoir by using dts temperature data in both production and shut-in periods in an offshore wellbore where esp pumps are located.

Methodology used:
The paper uses the software THERMA, which uses steady state pressure model together with transient thermal solutions, to evaluate temperature data. The software is adopted Darcy Law for vertical wells and Joshi Law for horizontal wells.

Conclusion reached:
Zonal contributions of different layers were determined. Also cross flow is detected during shut-in periods and production.

Comments:
For a long term reservoir evaluation by real time monitoring will be useful to detect cross flow and sand fill on the reservoir layers. These two phenomena extremely effects the reservoir performance and without analyzing temperature model, it is not possible to discover this problems.

SPE-109765 (2007)

A robust Steady-State Model for Flowing-Fluid Temperature in Complex Wells

Authors: Hasan, A.R., Kabir, C.S., Wang, X

Contribution to the understanding of analysis of temperature response to determine flow rates in producing zones:
The first model addressed to complex well temperature modelling. Although, there are available fluid temperature models are available for temperature profiling, this model offers temperature profile for highly deviated well scheme and multiphase flow.

Objective of the paper:
Calculation of flowing fluid temperature for deviated wells under steady state conditions for multiphase flow.

Methodology used:
Solving energy balance and thermodynamically defining each parameter for each phase, a robust model is developed to calculate flowing fluid temperature. This model is robust for multiphase flow under steady state conditions.

$$T_f = T_{ei} + \frac{1 - e^{(z-z_j)L_R}}{L_R}\left[g_G \sin\alpha + \varphi \frac{gsin\alpha}{c_p}\right] + e^{(z-z_j)L_R}(T_{f,j} - T_{ei,j})$$

Conclusion reached:
Three field example confirmed that the model can provide good temperature profile. The paper indicates that calculations from bottom to up is more accurate than top to bottom. Also, JTE heating effect can occur in highly pressured gas reservoirs.

Comments:
Since temperature is a function of mass flow rate, flow profiling can be performed using this approach to calculate zonal contribution of different layers. However, the model should be modified for different production sections since it models single point flow entry.

SPE-111790 (2008)

Modeling flow profile using distributed temperature sensors (DTS) system

Authors: Wang, X., Lee, J., Vachon, G.

Contribution to the understanding of analysis of temperature response to determine flow rates in producing zones:
This model is modified form of robust model of Hasan and Kabir for different production zones. It provides good approximation for estimating flow profile from different zones.

Objective of the paper:
The main objective is to model flow profile in the wellbore from different producing zones.

Methodology used:
Wellbore categorized into two parts which are producing and non-producing section. Heat transfer phenomena is solved for differently for production and non-production zone.

Non-Producing zone
Energy Equation

$$\frac{\mathrm{dH}}{dz} - \frac{gsin\alpha}{Jg_c} + \frac{vdv}{Jg_c dz} = -\frac{Q}{w}$$

Flowing fluid temperature

$$\frac{dT_f}{dz} = L_R\left(T_f - T_{ei}\right) + \left(\frac{gsin\alpha}{Jg_G c_p} - \varphi\right)$$

For Producing zone

Energy equation

$$-\mathrm{Q} = \mathrm{W}_1\left(\frac{\mathrm{dH}}{dz} - \frac{gsin\alpha}{Jg_c} + \frac{vdv}{Jg_c dz}\right) + W_2 c_p \frac{(T_f - T_{entry})}{dz}$$

Flowing fluid equation

$$\frac{dT_f}{dz} + \frac{(1-\lambda)}{\lambda}\frac{(T_f - T_{enry})}{dz} = \frac{L_R}{\lambda}\left(T_{ei} - T_f\right) + \left(\frac{gsin\alpha}{Jg_G c_p} - \varphi\right)$$

$$\lambda = \frac{W_1}{W_1 + W_2}$$

Conclusion reached:
The model shows good agreements both field and simulated data. As conclusion, JTE for high pressured gas wells shows heating instead of cooling effect.

Comments:

SPE-111790 (2008)

Modeling flow profile using distributed temperature sensors (DTS) system

Authors: Wang, X., Lee, J., Vachon, G.

Contribution to the understanding of analysis of temperature response to determine flow rates in producing zones:
This model is modified form of robust model of Hasan and Kabir for different production zones. It provides good approximation for estimating flow profile from different zones. In addition to previous publication, the study offers calculations for gas lift model.

Objective of the paper:
The main objective is calculation of temperature and flow profiling for a well producing with aid of gas lift.

Methodology used:
Wellbore categorized into two parts which are producing and non-producing section. Heat transfer phenomena is solved for differently for production and non-production zone. Regarding their previous work (SPE-11790) producing zone equation is adapted for gas mandrels.

Conclusion reached:
The model shows good agreements both field and simulated data. As conclusion, cooling effect of the injected gas is determined by the model.

Comments:

APPENDIX C

Governing Flowing Fluid Temperature for Single Phase Fluid.

To find flowing fluid temperature, the total energy and mass equations should be solved simultaneously but this solution can be approximated.[3] The total energy equation is represented as

$$dH + \frac{gdz}{g_c J} + \frac{udu}{g_c J} = dQ_t - \frac{dW_f}{J} \quad \text{(A-1)}$$

If this equation considered under steady state condition for a single phase fluid in constant boundaries so that work flow term W_f becomes zero and the Eq.A-1 becomes.

$$dH + \frac{gdz}{g_c J} + \frac{udu}{g_c J} = dQ_t \quad \text{(A-2)}$$

Governing Equation for Liquid Case

This derivation has been done for a non-compressible liquid hence, kinetic energy term is neglected then the equation forms

$$dH + \frac{gdz}{g_c J} = dQ_t \quad \text{(A-3)}$$

The change in total energy of a thermodynamic system is represented by enthalpy change. In this case it is a function of internal energy of the system, volume and pressure. Internal energy of the system can be represented by change in specific heat capacity by temperature. Therefore, the definition of enthalpy for a non-compressible fluid,

$$dH = dE + \frac{VdP}{J} = cdT + \frac{VdP}{J} \quad \text{(A-4)}$$

Internal energy is represented by following formula;

$$dE = cdT + \left[T \left(\frac{\partial p}{\partial T} \right)_V - P \right] dV \quad \text{(A-5)}$$

Considering fluid is non-compressible fluid and under the steady state conditions the expression becomes,

$$dE = cdT \quad \text{(A-6)}$$

While injected fluid moves down to the bottom hole, enthalpy increase due to increase in pressure and this change can be approximated by loss in the potential energy. In sense of energy conversation, it is valid for flowing up conversely. Loss in enthalpy is equals to gained potential energy by fluid.

$$dH = cdT - \frac{gdz}{g_c J} \quad \text{(A-7)}$$

Finally, subtracting eq. A-7 from eq. A-3 total energy equation is formed as follows

$$cdT = dQ_t \quad \text{(A-8)}$$

Assuming no phase change, heat rate lost by the mass of fluid is equals to heat transferred to unit area of casing wall.

$$dq = -WcdT_f = 2\pi r_{to} U (T_f - T_{co}) dz \quad \text{(A-9)}$$

Heat rate between casing wall and the formation can be expressed as a function of dimensionless time.

$$dq = \frac{2\pi k (T_{co} - T_e) dz}{f(t)} \quad \text{(A-10)}$$

To solve this equation we need to write T_{co} as a function of T_f. Hence, following steps need to be followed.

$$-WcdT_f = 2\pi r_{co} U (T_f - T_{co}) dz \quad \text{(A-11)}$$

$$T_{co} = T_f + \frac{WcdT}{2\pi r_{co} U dz} \quad \text{(A-12)}$$

After T_{co} is found as a function of T_f it is placed in the equations A-9 and A-10 and equalized to each other.

$$\frac{2\pi k(T_{co}-T_e)dz}{f(t)} = 2\pi r_{to}U(T_f - T_{co})dz$$ .... (A-13)

$$T_f - T_e = \left[\frac{Wc(r_{co}Uf(t)+k)}{2\pi U r_{to} k}\right]\frac{\partial T_f}{\partial z}$$ .... (A-14)

$$A = \left[\frac{Wc(r_{co}Uf(t)+k)}{2\pi U r_{to} k}\right]$$ .... (A-15)

$$\frac{T_f}{A} - \frac{T_e}{A} + \frac{\partial T_1}{\partial z} = 0$$ .... (A-16)

Geothermal temperature distribution is expressed as.

$$T_e = g_G z + T_{Gs}$$ .... (A-17)

Equation A-16 is nonhomogeneous first order differential equation. We can solve this by defining integration factor in A-18

$$u = e^{z/\mathrm{A}}$$

$$Q = \left(\frac{g_G z + T_{Gs}}{A}\right)\partial z$$ .... (A-18)

$$(\mathrm{u}\,\partial \mathrm{T}_f)' = Qu$$

$$T_f e^{z/\mathrm{A}} = \int \frac{(g_G z + T_{Gs})e^{z/\mathrm{A}}}{A} dz + C(t)$$ .... (A-19)

$$T_f e^{z/\mathrm{A}} = (\mathrm{g}_G\, z - \mathrm{g}_G\, A + T_{Gs})e^{z/\mathrm{A}} + C(t)$$ .... (A-20)

C(t) is evaluated at the injection or production point, where z=0, fluid temperature is equals to entry temperature.

$$C(t) = (T_0 + g_G A - T_{Gs})$$ .... (A-21)

Finally, fluid temperature flowing in the well after integrating equation A-19 and defining C(t) is expressed for injection well.

$$T_f(z,t) = g_G z + T_{Gs} - g_G A + (\mathrm{T}_0 + g_G A - T_{Gs})e^{z/\mathrm{A}}$$ .... (A-22)

For production well this equation can be modified by changing flowing down conditions to flowing up conditions. Hence Equation A-22 is modified as follows.

$$T_f\left(z,t\right) = T_{Ge} - g_G z + g_G A + \left(T_{fe} - T_{Ge} - g_G A\right)e^{-z/A}$$ .... (A-23)

APPENDIX D

Detailed demonstrations of field example calculations.

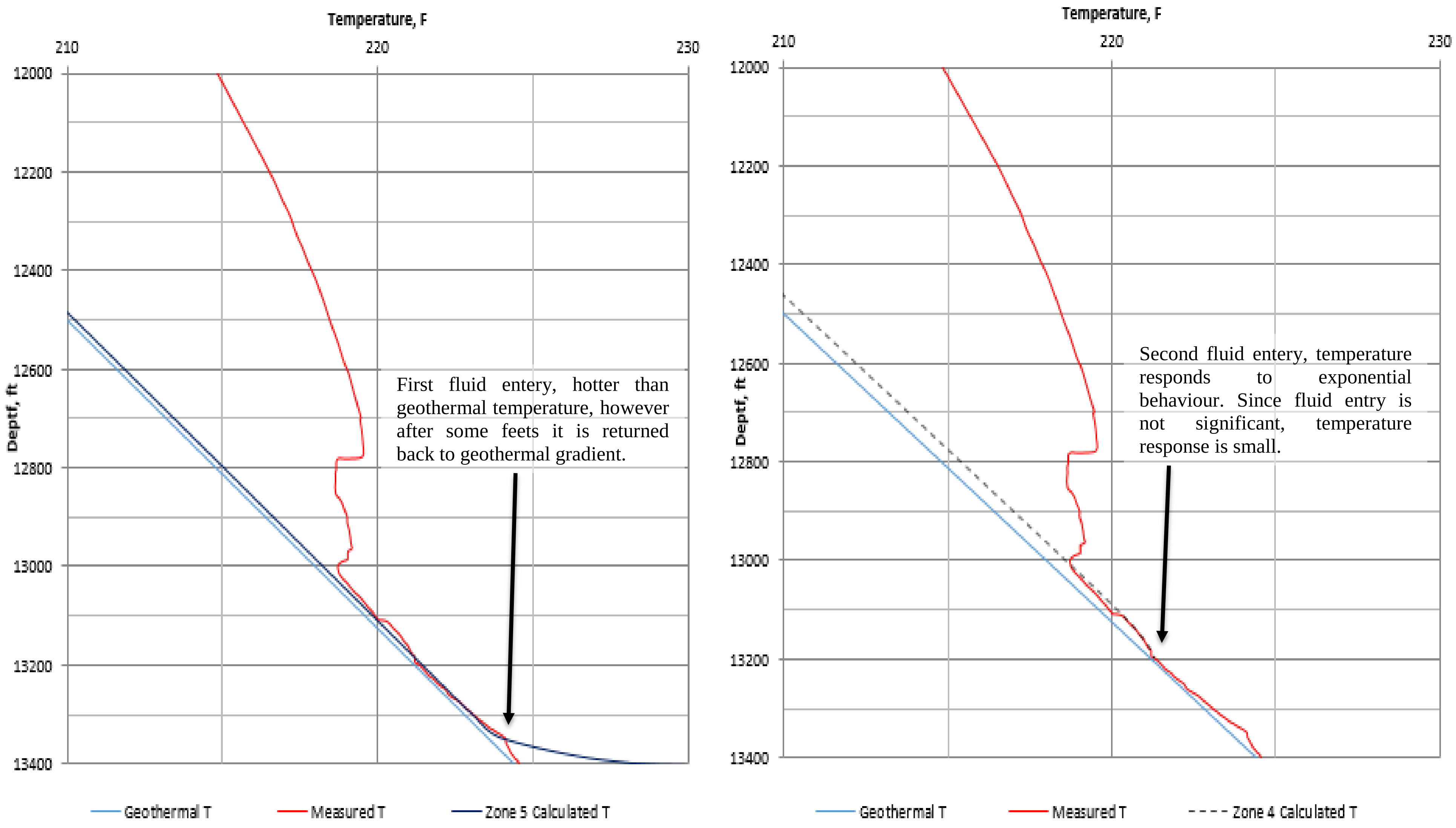

Figure 12: Field example 1, calculated temperature response of zone 1 and zone 2.

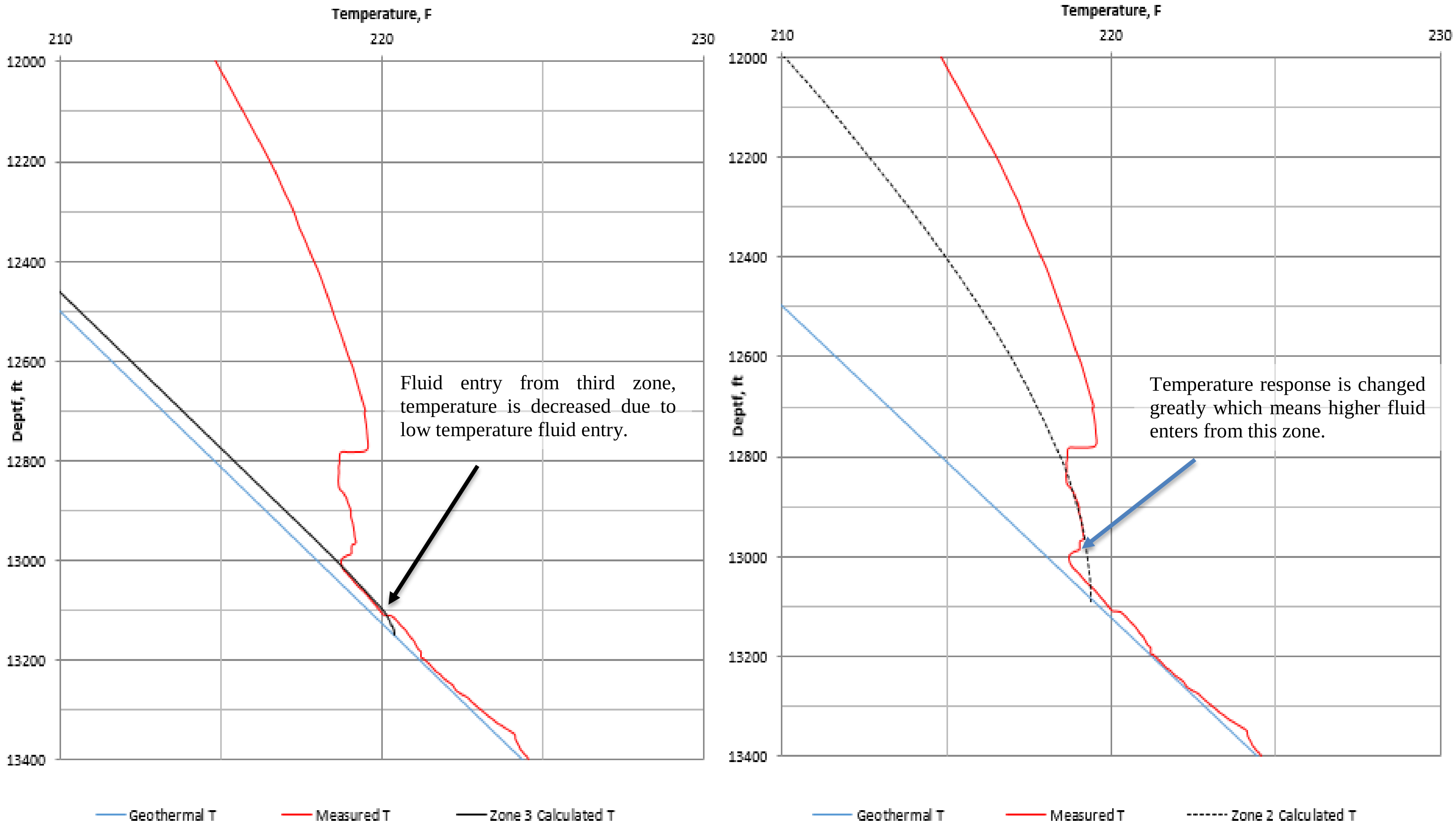

Figure 13: Field example 1, calculated temperature response of zone 3 and zone 4.

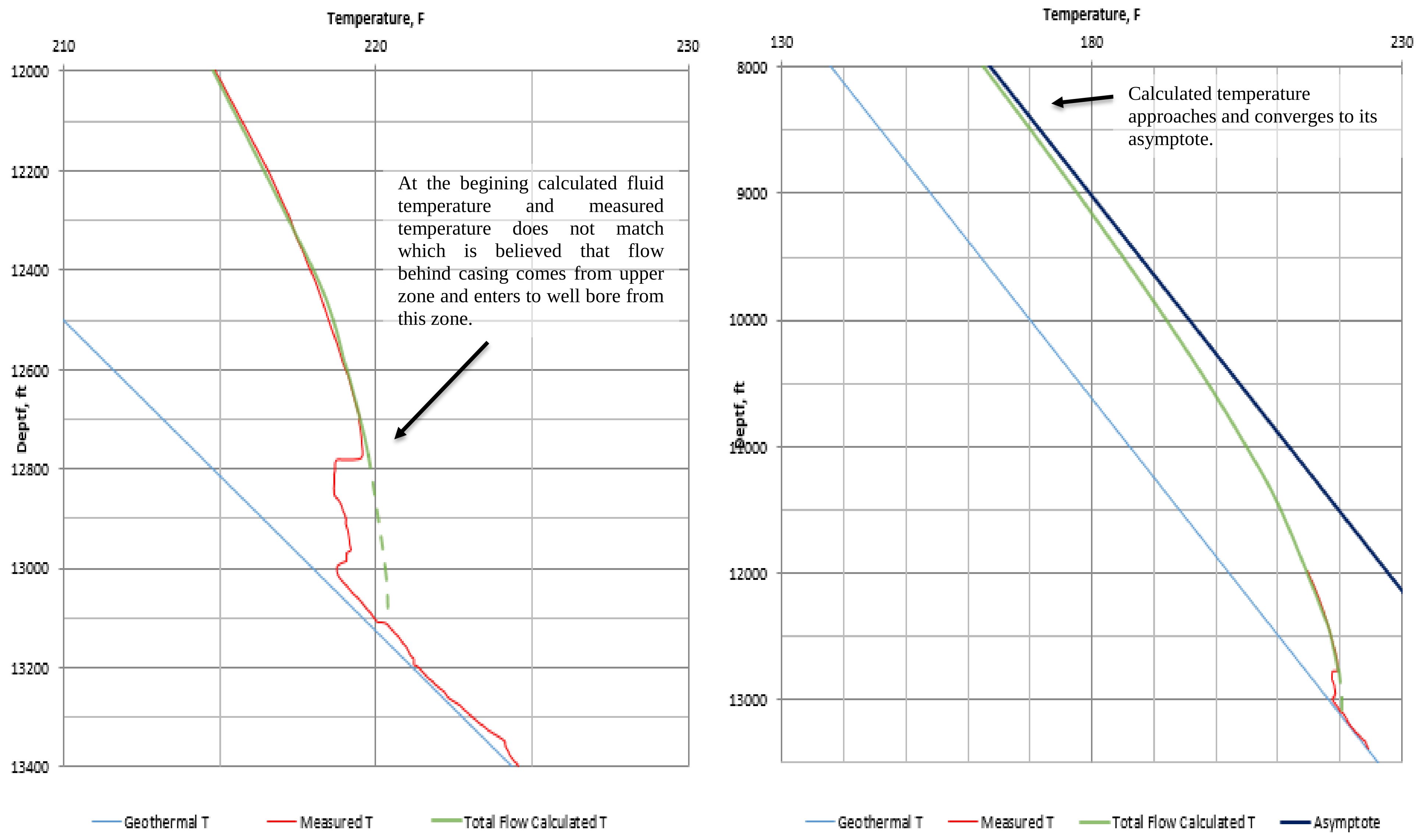

Figure 14: Field example 1, calculated temperature response of zone 5 and approaching temperature response of total flow to asymptote.

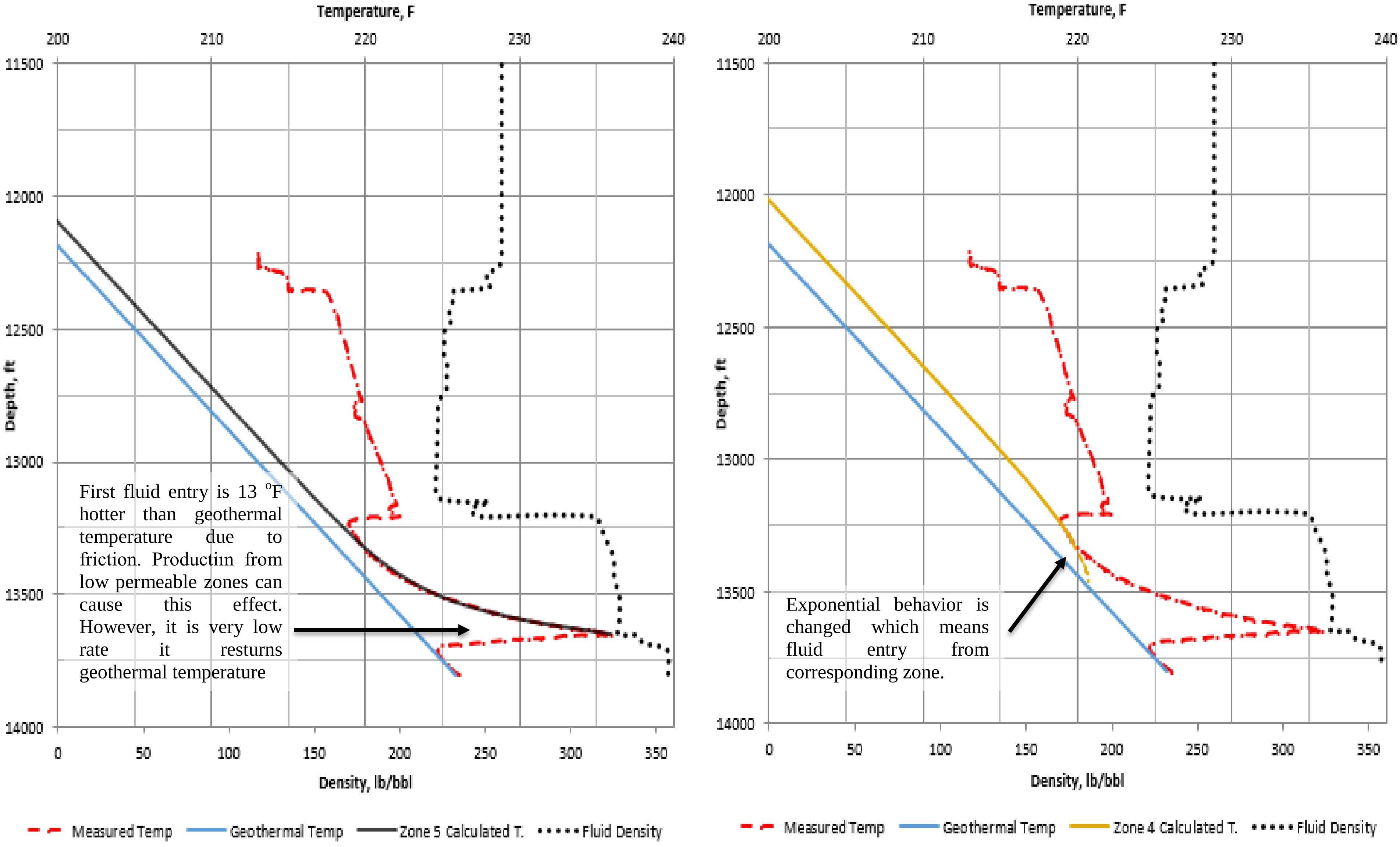

Figure 15: Field example 2, calculated temperature response of zone 1 and zone 2.

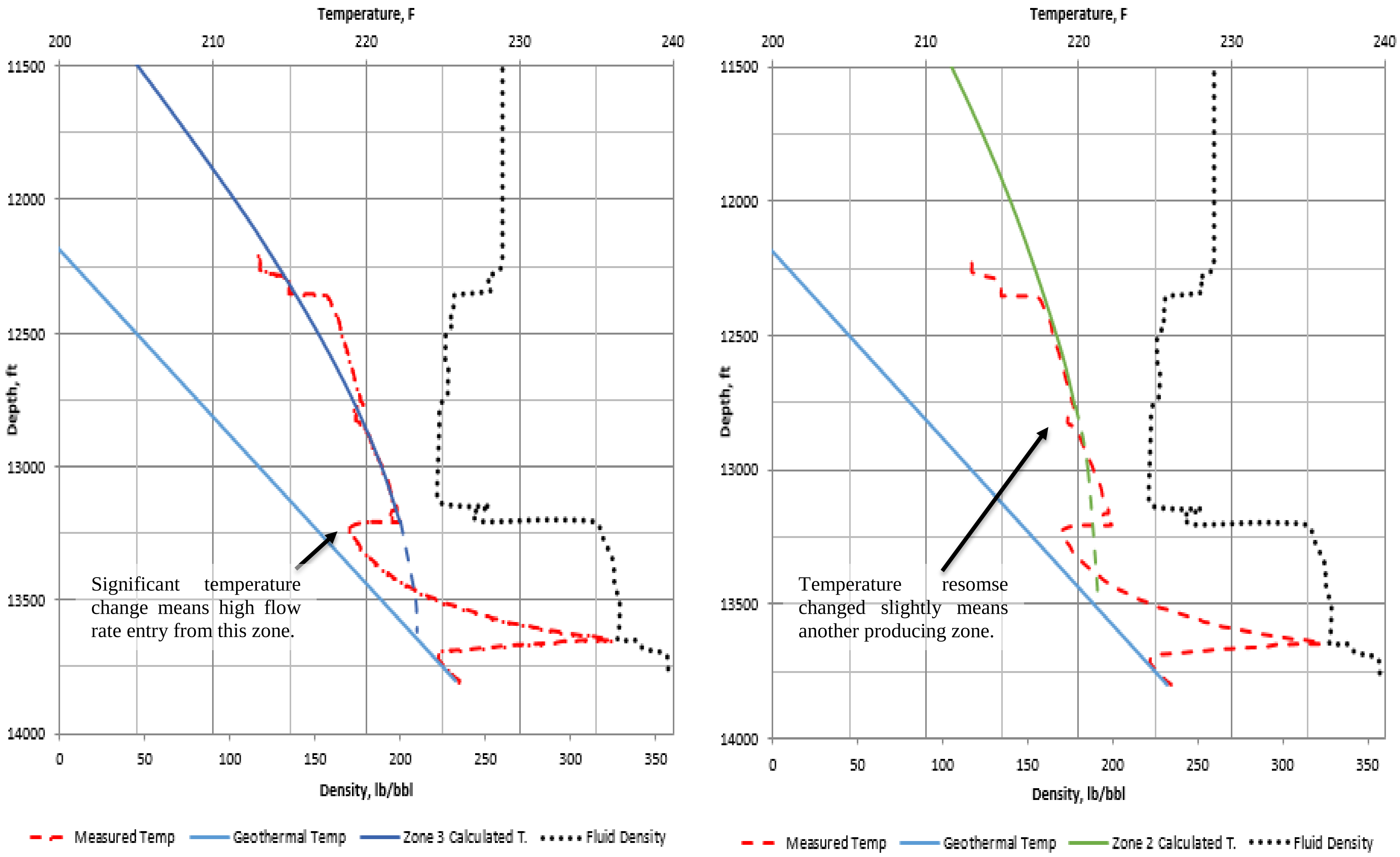

Figure 16: Field example 2, calculated temperature response of zone 3 and zone 4.

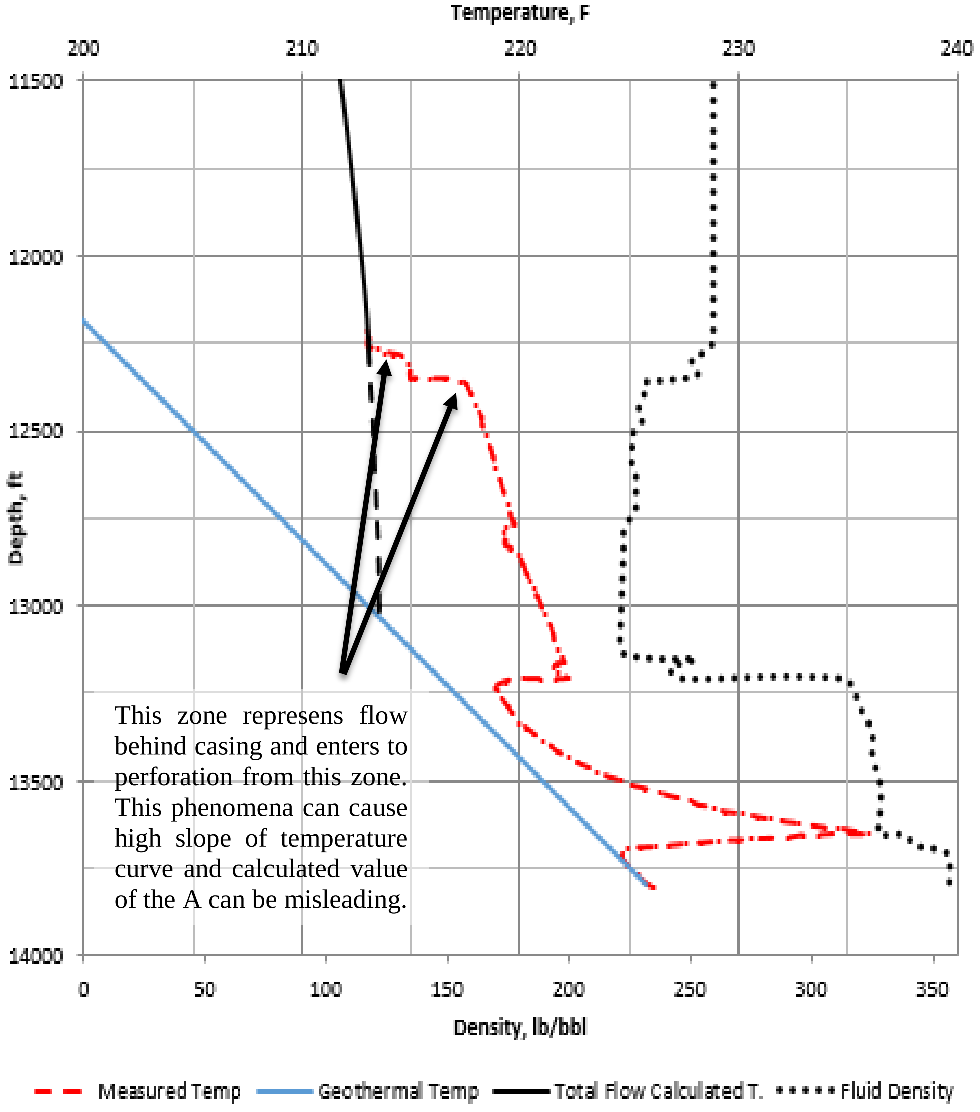

Figure 17: Field example 2, calculated temperature response of zone 5.